(12) INTERNATIONAL APPLICATION PUBLISHED UNDER THE PATENT COOPERATION TREATY (PCT)

(51) International Patent Classification:
G06T 5/00 (2006.01)         G06T 7/00 (2006.01)

(21) International Application Number:
PCT/US2007/024807

(22) International Filing Date:
3 December 2007 (03.12.2007)

(25) Filing Language:                          English

(26) Publication Language:                     English

(30) Priority Data:
11/612,711          19 December 2006 (19.12.2006)    US

(71) Applicant (for all designated States except US): CARE-STREAM HEALTH, INC. [US/US]; 150 Verona Street, Rochester, New York 14608 (US).

(72) Inventors; and
(75) Inventors/Applicants (for US only): RAY, Lawrence Allen [US/US]; 3861 Elmwood Avenue, Rochester, New York 14610 (US). SIMON, Richard A. [US/US]; 64 MacIntosh Drive, Rochester, New York 14626 (US).

(74) Common Representative: CARESTREAM HEALTH, INC.; 150 Verona Street, Rochester, New York 14608 (US).

(81) Designated States (unless otherwise indicated, for every kind of national protection available): AE, AG, AL, AM, AT, AU, AZ, BA, BB, BG, BH, BR, BW, BY, BZ, CA, CH, CN, CO, CR, CU, CZ, DE, DK, DM, DO, DZ, EC, EE, EG, ES, FI, GB, GD, GE, GH, GM, GT, HN, HR, HU, ID, IL, IN, IS, JP, KE, KG, KM, KN, KP, KR, KZ, LA, LC, LK, LR, LS, LT, LU, LY, MA, MD, ME, MG, MK, MN, MW, MX, MY, MZ, NA, NG, NI, NO, NZ, OM, PG, PH, PL, PT, RO, RS, RU, SC, SD, SE, SG, SK, SL, SM, SV, SY, TJ, TM, TN, TR, TT, TZ, UA, UG, US, UZ, VC, VN, ZA, ZM, ZW.

(84) Designated States (unless otherwise indicated, for every kind of regional protection available): ARIPO (BW, GH, GM, KE, LS, MW, MZ, NA, SD, SL, SZ, TZ, UG, ZM, ZW), Eurasian (AM, AZ, BY, KG, KZ, MD, RU, TJ, TM), European (AT, BE, BG, CH, CY, CZ, DE, DK, EE, ES, FI, FR, GB, GR, HU, IE, IS, IT, LT, LU, LV, MC, MT, NL, PL, PT, RO, SE, SI, SK, TR), OAPI (BF, BJ, CF, CG, CI, CM, GA, GN, GQ, GW, ML, MR, NE, SN, TD, TG).

Published:
—    with international search report

(54) Title: METHOD FOR SEGMENTATION OF LESIONS
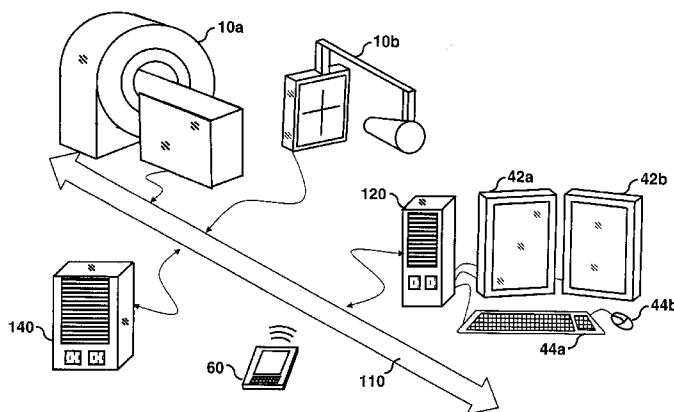
(57) Abstract: A method of segmenting a lesion (910) from normal anatomy in a 3-dimensional image comprising the steps of: receiving an initial set of voxels (520) that are contained within the lesion to be segmented; growing a region which includes the lesion from the initial set of voxels; identifying a second set of voxels (530) on a surface of the normal anatomy; determining a surface containing the second set of voxels which demarks a boundary (540) between the lesion and the normal anatomy; and classifying voxels which are part of the lesion.

# METHOD FOR SEGMENTATION OF LESIONS

## FIELD OF THE INVENTION

The present invention relates to the field of digital imaging, and

5    more particularly to processing a digital image to segment an object in a 3-
dimensional data set.

## BACKGROUND OF THE INVENTION

Identification of potentially cancerous lesions in CT and MRI
studies is a common task of radiologists. An important aspect of this task is

10   determining the extent and the volume such a lesion occupies. This is a tedious
task to accomplish manually, due to the irregular shape of suspected lesions and
the ever-increasing number of slices captured by diagnostic imaging systems.

A method of automating the process is to have a computer perform
such a task once the lesion has been identified. This task is commonly referred to

15   in the image-processing domain as image or volume segmentation and techniques
referred to as region growing are typically applied. Region growing algorithms
typically use local image characteristics, such as image intensity variations to
decide whether a neighboring voxel (3D volume images) or pixel (2D planar
images) is to be added to the growing region. However, segmenting lesions from

20   normal anatomy is a difficult task, (see Hong Shen, et. al., "A New Algorithm for
Local Surface Smoothing with Application to Chest Wall Nodule Segmentation in
Lung CT Data," Medical Imaging 2004, Proceedings of SPIE Vol. 5370) as the
image differences the lesion and normal anatomy often are not discernable in
terms of voxel intensity values, e.g., Hounsfield units HU. As a consequence,

25   region-growing tasks often expand beyond the target and, in the case of
segmenting lesions, include regions that are most likely to be healthy tissue or
normal anatomy.

The subsequent phase is to ascertain a surface that separates the
lesion from normal anatomy within the initial segmented region. Common

30   approaches to the problem are to fit a plane or low degree polynomial surface, or a
sequence of dividing lines on a slice-by-slice basis, to demark the boundary
between normal anatomy and the suspected lesion. Unfortunately, these methods

are too restrictive and often fail to produce desirable results. A primary reason is that such approaches are overly simplistic and do not account for the local geometry, or the variability of surfaces within a volume. The selection of a surface model imposes an implicit assumption on the kind of local surface one

5      expects.

The present invention approaches this problem by using methods that overcome these limitations. The invention is an ensemble of methods, where each is increasingly sophisticated, but requires more computational resources. All of these methods use the boundary of the leading edge of an expanding

10     segmentation front that is likely to be part of the normal anatomy and finds a surface that holds this boundary fixed.

## SUMMARY OF THE INVENTION

It is an object of the present invention to ascertain a surface that separates the lesion from normal anatomy within the initial segmented region,

15     such as a pulmonary lesion, from the background tissue in a volumetric medical image. More particularly, the object is to refine segmentation in cases using knowledge of normal anatomy.

Briefly, according to one aspect of the present invention a method of segmenting a lesion from normal anatomy in a 3-dimensional image

20     comprising the steps of: receiving an initial set of voxels that are contained within the lesion to be segmented; growing a region which includes the lesion from the initial set of voxels; identifying a second set of voxels on a surface of the normal anatomy; determining a surface containing the second set of voxels which demarks a boundary between the lesion and the normal anatomy; and classifying

25     voxels which are part of the lesion.

The present invention has an advantage of determining a boundary between a lesion and tissue initially identified as a lesion by an image segmentation algorithm. In particular, the present invention separates normal anatomy from structures of pulmonary lesions. The separation is done in

30     accordance with local anatomical geometry and does not impose a low level ad hoc parametric model for the task.

## BRIEF DESCRIPTION OF THE DRAWINGS

Figure 1 is a diagram showing a medical imaging communications network of connected computers suitable for practicing the present invention;

Figure 2 is block diagram showing the details of the software program running within the diagnostic workstation computer;

Figure 3 is block diagram showing the details of the lesion segmenter;

Figure 4 is block diagram showing the details of the initial lesion segmenter;

Figures 5a, 5b, and 5c is a schematic representation of the segmentation process within the initial lesion segmentor;

Figure 6 shows a graph of the number of voxels as a function of path length for different idealized lesion types.

Figure 7 is diagram showing the segmentation fronts generated by the region growing processing;

Figure 8 shows the parent-child relationship between segmentation fronts;

Figures 9a and 9b depict a 3D representation of a lesion attached to the lung wall;

Figure 10 depicts the transformation of the local coordinates of a surface patch;

Figures 11a, 11b, and 11c depict a 3D representation of segmentation fronts on the lung wall;

Figure 12 depicts the 2D location of surface constraints for a lesion attached to the lung wall; and

Figure 13 is block diagram showing the details of normal anatomy/lesion separator.

## DETAILED DESCRIPTION OF THE INVENTION

Many medical imaging applications are implemented via a picture archiving and communications systems (PACS). These systems provide a means

for displaying digital images acquired by a wide variety of medical imaging modalities such as, but not limited to, projection radiography (x-ray images), computed tomography (CT images), ultrasound (US images), and magnetic resonance (MR images). Each of the above mentioned medical imaging

5   modalities contain a slightly different set of diagnostic information. In particular, CT and MR images are obtained with imaging x-ray emission and when viewed and studied by radiologist, can reveal much detail about a patient's 3-dimensional internal anatomy. Computer algorithm technology can also be applied to medical images to enhance the rendering of the diagnostic information, to detect an

10  abnormal condition, i.e. computer aided detection (CAD), and to make measurements relating to the patient's condition, i.e. computer aided measurement (CAM).

The present invention represents an algorithmic computer method for segmenting a portion of a medical image with anatomical relevance. In

15  particular, the primary motivation for the development of the technology described herein is the segmentation of abnormal pulmonary lesion tissue from normal pulmonary tissue. An intended use for the herein described technology is as follows. A radiologist reviews a thoracic CT exam on a medical PACS and indicates to the CAM segmentation software the position of a suspected

20  pulmonary lesion. The voxel position indicated represents a seed point assumed to be part of the pulmonary lesion. The CAM segmentation software then identifies the voxels surrounding and contiguous with the seed point that are also associated with the pulmonary lesion. Once the region associated with the pulmonary lesion has been segmented a corresponding volumetric size can be

25  calculated. The technology advancement of the present invention relates to the particular method of performing the image segmentation task. For the purpose of the description herein, the terms lesion and nodule are synonymous and should be considered interchangeable.

In the following description, a preferred embodiment of the present

30  invention will be described as a software program. Those skilled in the art will readily recognize that the equivalent of such software may also be constructed in hardware. Since image processing and manipulation algorithms and systems are

well known, the present description will be directed in particular to algorithms and systems forming part of, or cooperating more directly with, the method in accordance with the present invention. Other aspects of such algorithms and systems, and hardware and/or software for producing and otherwise processing
5       the image signals involved therewith, not specifically shown or described herein may be selected from such systems, algorithms, components, and elements known in the art. Given the description as set forth in the following specification, all software implementation thereof is conventional and within the ordinary skill in such arts.

10              A system suitable for practicing the present invention is illustrated in Figure 1 showing a medical imaging communications network that includes multiple connected computers. Such a network of computers provides a means of sending and receiving information between any two or more connected computers. The image capture device 10a symbolically represents a number of
15      medical digital image modality devices such as, but not limited to, a computed tomography scanning device (CT) or magnetic resonance imaging scanning device (MR) that is capable of producing 3-dimensional digital images of patient anatomy. The 3-dimensional digital images are typically composed of a series of cross-sectional, or slice, images through the patient anatomy.

20              Also connected to the communications network 110 is a digital radiographic (DR) capture device 10b capable of producing digital x-ray images. As such, the images produced by a DR capture device typically are one or more 2-dimensional digital images each representing a different exposure and or imaging path through the patient. For example, the DR capture device 10b can be used to
25      acquire multiple projection radiographic digital images with its x-ray source located in different positions relative to the patient. The resulting DR radiographic digital images can be processed to produce a set of slice digital images that represent a 3-dimensional digital image of the patient.

              The slice digital images (not shown) produced by the capture
30      device 10a are transmitted via the communications network 110 to a image archive computer 140 where, along with patient history information, they become part of an electronic patient history record. The main function performed by the

image archive computer 140 is the facilitation of transfer or exchange of image information rather than the processing of information. The image archive computer 140 serves as a large storage repository of digital images and other medical information. The arrows in the diagram of Figure 1 represent the

5    exchange of information, which in general, is bi-directional, i.e. the flow of information can be in either direction.

The slice images are later queried on a diagnostic workstation computer 120, sometimes referred to as a picture archive and communication system (PACS), for viewing and examination by a radiologist or similarly trained

10   medical professional. The diagnostic workstation computer 120 can have multiple electronic displays connected for viewing medical images. Two such electronic display devices 42a and 42b are shown in Figure 1. Also connected to the diagnostic workstation computer 120 are input devices 44a and 44b depicted here as keyboard and mouse devices respectively. Although the technology of the

15   present invention was envisioned as operating within the context of a diagnostic workstation computer, it should be noted that any computing device capable of displaying and processing image data could be used. In particular, a mobile computer 60 shown in Figure 1 can be used with the present invention. Thus, it is not necessary for the computer to be physically connected to the communications

20   network 110.

A PACS can be defined as a system that acquires, transmits, stores, retrieves, and displays digital images and related patient information from a variety of imaging sources and communicates the information over a network. By this definition, the diagnostic workstation computer 120 shown in Figure 1 can

25   represent a PACS. Similarly, the combination of the diagnostic workstation computer 120, mobile computer 60, image archive computer 140, and communication network 110 can collectively be considered a PACS. In addition to the patient digital images, PACS transmit, receive, and store other electronic patient record information such as, but is not limited to, non-image information

30   (meta-data) such as age, sex, medical history, prescribed medications, symptoms, etc.

For the purposes of the discussion of the present invention the collection of inter-connected computers including the communications network will be also be referred to as a DICOM network since DICOM formatted digital images are currently the most prevalent file encoding used for medical digital

5      images. Typically a 3-dimensional volume image is constructed from set of 2-dimensional slice digital images wherein each slice digital image is encoded as an individual DICOM file.

Often an individual image data element, i.e. single value representing signal intensity at a point or small region, is referred to as a voxel for

10     3-dimensional images and a pixel for 2-dimensional images. The term voxel is commonly used to characterize a volume-element whereas the term pixel is commonly used to characterize a picture-element. The technology embodied within the present invention can be applied to 2-dimensional and 3-dimensional images. As such, for the purposes of the description herein, the terms voxel and

15     pixel should be considered interchangeable, i.e. describing an image elemental datum capable of having a range of numerical values. Voxel and pixels can be said to have the attributes both of location and value.

With the medical imaging system setup as described above and shown in Figure 1, a medical professional such as a radiologist (not shown), uses

20     the keyboard 44a or mouse 44b to indicate to the software application program 150 (shown in Figure 2), running on the diagnostic workstation computer 120, the desired patient record (not shown) to be loaded into memory. The CT digital image exam, i.e. the set of CT slice digital images, is then retrieved from the image archive computer 140 and displayed on the electronic display devices 42a

25     and/or 42b. After viewing the image data, the medical professional indicates to the system the location of a suspected pulmonary lesion with a click of the mouse, input device 44b. Typically this is performed by sequentially scrolling through the 2-dimensional slice images and viewing the slice digital image that best shows the suspected pulmonary lesion.

30     A brief overview of the flow of image information into, out of, and within segmentation application program, referred to as the "segmenter" 150 is depicted by Figure 2. The segmenter 150 receives a set of source digital images

7

201, a seed point 205, and image processing parameters 206 and produces a reported volume 207, a segmentation map 204, and alternatively, a rendered segmentation map 209, using image renderer 240. Within the segmenter 150, the following analysis and processing is performed. The slice image assembler 220

5    receives the multiple images as the set of source digital images 201 and generates a volume image 202. The volume image 202, the image processing parameters 206, and the seed point 205 are then passed to the lesion segmenter 230, image renderer 240, and volume estimator 250. The volume image 202 provides imaging voxel data regarding the 3-dimensional nature of the patient anatomy.

10   The image processing parameters 206 contain multiple data items that regulate, or control, the actions of the lesion segmenter 230. The seed point 205 communicates location of a suspected pulmonary lesion. The lesion segmenter 230 generates a segmentation map 204, i.e. volume image data that indicates, on a voxel by voxel basis, the segmentation classification information as to whether or

15   not each voxel is considered part of the segmented lesion or another anatomical structure.

The details of the lesion segmentor 230 shown in Figure 2 are depicted in more detail in Figure 3. The lesion segmentor 230 produces, on output, a final segmentation map 204 that represents the voxels identified as part

20   of the pulmonary lesion, spiculated tentacle's of the lesion, vessels, normal anatomy (lung wall, mediastinum, etc), background (lung parenchyma). The initial lesion segmentor 310 receives the volume image 202, seed point 205 and image processing parameters 206 as input and produces segmentation front paths 208 and the initial segmentation map 203. The image processing parameters 206

25   are a set of control parameters used to regulate the overall segmentation processing. The seed point 205 indicates an x, y, z location (typically as a set of i, j, k indices) of a suspected pulmonary lesion within the volume image 202. It is about this voxel location that the initial lesion segmentor 310 performs a first segmentation process. Optionally, the location of the seed point can be

30   automatically adjusted to ensure the segmentation result is independent of the seed point location; as long as the seed point is inside the lesion. The initial segmentation map 203 represents a first-attempt classification of voxels, by the

initial lesion segmentor 310, for voxels classified as part of the pulmonary lesion. A segmentation front path is a collection of voxels that represent a connected region-growing sequential path that is generated as part of the region growing processing. The ensemble of segmentation front paths 208 is a catalog of all the individual segmentation front paths. The segmentation front path analyzer 320 receives the segmentation front paths 208 and classifies each individual segmentation front path as associated with a particular anatomical structure. The segmentation map refiner 330 using both the segmentation front paths 208 and the initial segmentation map 203 and performs further refinement of the segmentation processing. The segmentation front path analyzer 320 classifies those voxels associated with non-lesion anatomy structures. The final segmentation map 204 incorporates these refinements. The final segmentation map 204 identifies voxels deemed to be part of the lesion tissue and voxels that are part of non-lesion anatomy. The embodiment of lesion segmentor 230 as describe within is referred to as a segmentation front analysis.

The details of a preferable initial lesion segmenter 310 shown in Figure 3 are depicted in more detail in Figure 4 and schematically in Figures 5a, 5b, and 5c. Without loss of generality, the schematic representation of the lesion segmentor in Figures 5a, 5b, and 5c represent a two-dimensional embodiment where the grid 500 has been uniformly sampled and connectivity of four grid elements (pixels) have been assumed. One skilled in the art will realize that the above representation can be extended to three or more dimensions with different degrees of connectivity between grid elements (voxels). Upon initiation the initial lesion segmentor 310 receives the volume image 202, seed point 205, and image processing parameters 206 as input. The set of voxels 520 on the boundary of the current segmentation map 510 are denoted as the current segmentation front from which further growth of the segmentation can occur. Initially the set of voxels in the segmentation is the seed point 205 and is considered the first segmentation front. In the grow segmentation step 312, the segmentation region grows by adding a set of voxels 530, according to a predefined set of rules, starting from the set of voxels 520 on the boundary of the current segmentation map 510. The number of voxels added to the segmentation during the grow segmentation step

312 is controlled by D1; a parameter in the image processing parameters 206. In a preferred implementation of the initial lesion segmentor 310, during the grow segmentation step 312 at a minimum every voxel on the boundary of the current segmentation 510 is used to grow the segmentation region. The set of voxels 530 is added to the current segmentation map 510 producing segmentation map 510a that subsequentially becomes the current segmentation map.

In the classify segmentation front into active and inactive fronts step 313, the current segmentation front is delineated and is classified into active 540 and inactive 550 segmentation fronts. Inactive segmentation fronts contain voxels in which no further growth of the segmentation can occur according to the segmentation criteria. Segmentation fronts that contain voxels that can initiate further growth are considered active fronts. In the partition active segmentation front into connected fronts step 314, the active segmentation front is partitioned into a set of uniquely labeled connected fronts 540a and 540b where all the voxels of a uniquely labeled front are connected.

In the calculate features for each connect front step 315, features for each segmentation front are computed. Features for each segmentation front $k$ and the volume associated with each segmentation front can be computed, such as, the number of voxels $N_k$, the center of gravity (centroid) $C_k$, shape and orientation, direction between successive segmentation fronts, curvature, etc. The centroid of a wave-front part is defined as

$$\mathbf{C}_k = \frac{1}{N_k} \sum_i \mathbf{X}_i$$

where $\mathbf{X}_i$ is the coordinate of the $i$th voxel in segmentation front $k$. The direction between successive segmentation front is defined as

$$\mathbf{D}_k = \mathbf{C}_{k+1} - \mathbf{C}_k$$

and the curvature is defined as

$$\kappa_k = \left| \mathbf{D}_k - \mathbf{D}_{k-1} \right|.$$

The shape and orientation of the $k$th segmentation front can be determined by the eigenvalues $\lambda$ and eigenvectors u of the covariance matrix of the voxel's spatial

coordinates X that makeup the k*th* segmentation front. The eigenvectors yield the orientation or principal axes of the front and eigenvectors yield information related to the shape of the front. For example, if eigenvalues are ordered in magnitude such that $\lambda_1 \leq \lambda_2 \leq \lambda_3$, then a front associated with a vessel is

5    indicated by $\lambda_1$ being small (ideally zero), and $\lambda_2$ and $\lambda_3$ are of larger and similar magnitude. The respective eigenvectors $\mathbf{u}_1$ indicates the direction along the vessel and $\mathbf{u}_2$ and $\mathbf{u}_3$ form the normal (orthogonal) plane.

In the link connected fronts with segmentation front paths step 316, each labeled connected front is linked into a parent-child relationship with a

10   previous labeled segmentation front generating a segmentation front path. A segmentation front path is the list of distinct segmentation fronts traversed, starting from the seed point 205, in which successive segmentation fronts are linked together by a parent child relationship. Hence a data-structure in the form of a tree is created where each segmentation front path represents a unique path

15   through the tree structure.

In the continue segmentation step 317, a decision is made whether to continue looping through the segmentation process. One way the processing can finish is if there are no active segmentation fronts available for further segmentation growth. Another way the processing can terminate is if the

20   segmentation front paths indicate that the only current segmentation growth is occurring within normal anatomy, see below. The loop processing within the initial lesion segmentor 310 can also be stopped if a condition specified by parameter value D2 contained in the image processing parameters 206 is meet. For example, the total number of voxels contained in the segmentation map has

25   exceeded a given threshold. When the loop processing has finished, the current segmentation map becomes the initial segmentation map 203. At this stage, voxels within the initial segmentation map 203 are classified either as being lesion or background.

A preferred embodiment of the initial lesion segmentor 310

30   employs a version of the Fast-Marching method described by J.A. Sethian in the publication "Level Set Methods and Fast Marching Methods", Cambridge

University Press, 1999. The fast marching approach models the segmentation process as a propagating wave front, a surface in 3D or a curve in 2D, which over time is moved by image and non-image driven forces to the boundaries of the desired objects. The wave front corresponds to the segmentation front defined

5    previously. The propagating wave front may be described by the eikonal Equation,

$$\left(\frac{\partial t}{\partial x}\right)^2 + \left(\frac{\partial t}{\partial y}\right)^2 + \left(\frac{\partial t}{\partial z}\right)^2 = \frac{1}{s^2(x,y,z)} = c(x,y,z) \qquad (1)$$

where $t$ is the time at which the front crosses point (x, y, z), $s$ is the speed

10   function, and c is the cost function.

The fast marching method solves Equation (1) by directly mimicking the advancing wave front. Every point on the computational grid is classified into three groups: points behind the wave front who have already been segmented, whose travel times are known and fixed; points on the wave front,

15   whose travel times have been calculated, but are not yet been segmented; and points ahead of the wave front. The algorithm then proceeds as follows:

1) Choose the point on the wave front with the smallest travel time.

2) Fix this travel time.

20   3) Advance the wave front, so that this point is behind it, and adjacent points are either on the wave front or behind it.

4) Update the travel times for adjacent points on the wave front by solving Equation (1) numerically.

5) Repeat until every point is behind the wave front or until a

25   stopping condition has been meet.

Many different cost-function can be used in the context of a fast-marching approach. For example, the cost-function can be based on the magnitude of the gradient of voxel values. Another cost-function can be based on the curvature of surface normal vectors. Additionally, any combination of cost-

30   functions can serve as cost-function. A preferred embodiment used a binary cost-

function that returns 1 for voxels whose value is above a given threshold and infinity for voxels whose value is below or equal to the threshold. By choosing a cost function that returns infinity for a voxel value below the threshold results in the inactivation (or freezing) of the segmentation front at that voxel. This type of

5      cost function yields a geodesic distance map that associates each voxel within the segmentation with its geodesic distance from the seed point 205. A threshold value of approximately -350 HU works well for segmenting solid-type pulmonary lesions. The cost-function threshold value, included in the image processing parameters 206, can be a parameter that is application specific or even

10     preferentially set by an individual radiologist. Alternatively, the threshold can be determined automatically by an algorithmic method. For example, the threshold can be determined either by analyzing traces of the voxels values that originate at the seed point and extend in different directions through the nodule to the background (lung parenchyma) or by histogram analysis of voxel values in a

15     bounding volume about the seed point that is large enough to include the both nodule and background. In a preferred implementation of the fast marching approach, parameter values D1 and D2 contained in the image processing parameters 206 respectively represent an increment in the geodesic distance traveled from the current segmentation front to a voxel and the geodesic distance

20     from the seed point 205 to an active segmentation front. In the preferred implementation the incremental geodesic distance between segmentation fronts controlled by D1 is set equal to one and the total geodesic distance traveled before stopping initial lesion segmentor 310 controlled by D2 is set equal to 40 mm.

One skilled in the art will recognize that there are many different

25     algorithms that can be used to calculate a geodesic distance map or a cost weight variant of geodesic distance map that can be utilize in the current invention.

The initial lesion segmentor 310 often expands beyond the target and in the case of segmenting lesions, can include regions that correspond to normal anatomy. There are many types of pulmonary lesions that can be

30     distinguished by the analysis of the segmentation front paths 208. The segmentation front paths 208 can be use to ascertain regions that correspond to normal anatomy and to generate surfaces that separate the lesion from normal

anatomy within the initial segmented region. Referring to Figure 3, the
segmentation front paths 208 generated by the initial lesion segmentor 310 are
analyzed for structural characteristics by the segmentation front path analyzer 320.
The features computed in step 315 are used to analyze the segmentation front

5      paths or sections of a segmentation front path. For many cases, a plot of the
number of voxels in a segmentation front plotted for successive segmentation
fronts reveals much about the underlying anatomical structure. For isotropically
sampled voxel data, the number of voxel relates directly to the surface area of a
segmentation front. For anistropically sampled voxel data, the number of voxels

10     in the segmentation front can be used as a surrogate for the surface area.

Idealized plots for a sessile juxta-pleural lesion 610, a juxta-
vascular lesion 620, a juxta-vascular lesion attached via a vessel to another
anatomical structure 630, and a lesion containing a spiculated tentacle 640 are
shown in Figure 6. In the sessile juxta-pleural lesion 610, when the advancing

15     segmentation front path penetrates into the lung wall or mediastinum, the
progression of surface area values starts to increase substantially (approximately
squared distance relationship) as a function of path-length (geodesic distance from
the seed point 205 to a given segmentation front). An unrestrained segmentation
front surface will have a corresponding surface area progression that varies

20     approximately as the distance squared. This situation can happen if a seed point is
located within a solid mass.

Another anatomical structure that can be differentiated by
analyzing the properties of the segmentation front is a spiculated tentacle 640. As
shown in the graph depicted in Figure 6, the surface area, or number of voxels, of

25     the progression diminishes with path-length until, eventually, the progression
terminates. Most spiculated tentacles vanish in just a short path length.
Conversely, vessels (juxta-vascular 620) tend to have corresponding progressions
of surface area that are relatively constant as a function of path-length.
Additionally, larger vessels have correspondingly greater number of voxels and

30     larger surface area values. The surface area of the segmentation fronts that
correspond to vessels essentially represents the cross-sectional area of the vessel
since the segmentation front surface progression tends to follow the axis of

vessels. By observation, most spiculated tentacles have smaller corresponding surface area values associated with their respective segmentation fronts.

Lesions, especially cancerous lesions, can grow along vessels and form spiculated tentacles that connect to another anatomical structure. When a

5      lesion is connected to another structure, e.g. another lesion, the chest wall or heart, the progression of surface area values, or number of voxels, can initially diminish as a function of path-length and then increase. The increase in the surface area value corresponds to the segmentation front surface passing the intersection point with a different anatomical structure. If the segmentation front of a segmentation

10     front path progress along a vessel, the corresponding surface area values can stay relatively constant (while in the vessel) and then increase when a larger anatomical structure is intersected as shown in the graph of Figure 6. For the case of a pedunculated juxta-pleural lesion, the progression of surface area values corresponding to the pedicle structure can be constant, diminish, diminish and

15     then increase, or just increase. However, when the corresponding segmentation front progresses past the intersection with the chest wall, the progression embarks on an approximately squared distance relationship as described above.

The segmentation front paths or sections of a given segmentation front path are classified by the manifestation of predetermined relationships

20     between successive segmentation fronts of a given segmentation front path. The simplest method for distinguishing different types of segmentation front paths from the other types includes using thresholds, range limits, and trend lengths on the number of voxels. An alternative method involves analyzing the number of voxels in the segmentation front path to determine the rate of increase in the

25     number of voxels as a function of the path-length. Vessel-like structures can be identified by examining the plot of the number of voxels in each segmentation front of a segmentation front path, see Figure 6, for regions where the number of voxels in a segmentation front is below a predetermined threshold and is approximately constant for a minimum given path length. In addition the vessel-

30     like structures can further be identified by examining the shape parameters and directions for each segmentation front for consistency between each segmentation front and consistency with a prior vessel model. Spiculated tentacle-like

structures are identified in a similar way by looking for a diminishing progression of number of voxels over a relatively short length with termination. The segmentation fronts and voxels that occur after the identified segmentation front that starts vessel-like structure are classified as vessel (or spiculated tentacle).

5          Lesions that are attached to large normal structures such as the pleural wall or mediastinum are identified by looking for region where the progression of number of voxels in a wave front part are increasing at a large rate for a relatively long path length, see Figure 6. When a wave-front part progresses to the stage that it includes roughly 1000 voxels, it is very likely to have

10  intersected with a large anatomical structure. Once this type of segmentation front path has been identified it is necessary to determine where (i.e. at which segmentation front) the intersection between the lesion and large anatomical structure has occurred. In many instances it has been observed that when the segmentation front penetrates a large anatomical structure that ratio of the number

15  of voxels in successive segmentation front is greater than would be expected based upon a squared distance relationship. An approximate boundary between the lesion and normal anatomy is given by the aforementioned segmentation front. The segmentation fronts and voxels that occur before the identified large anatomical structure are classified as lesion type. The segmentation fronts that

20  occur after the large anatomical structure are classified as normal anatomy. If deemed necessary more sophisticated methods can be used to demark the boundary between the lesion and normal anatomy. For example, the intersection points between the identified segmentation front and the boundary between anatomical structure and lung parenchyma can be identified and used to fit a 3

25  dimensional plane. The segmentation fronts and voxels that occur on the side of the plane containing the seed point are classified as lesion type. The segmentation fronts and voxels that occur on the side of the plane not containing the seed point are classified as normal anatomy and can be removed from the segmentation map.

Figure 7 shows a schematic 2-dimensional representation of a

30  lesion that is both a sessile juxta-pleural and juxta-vascular lesion and the resulting segmentation fronts produced by the initial lesion segmentor 310. The segmentation front 705, 710, 715, 735, 740, and 745 represents a single

segmentation front path for a sessile juxta-pleural lesion type and segmentation
fronts 705, 710, 715, 720, 725, and 730 represents a segmentation front path for a
vessel. Figure 8 shows the parent-child relationship of the segmentation fronts in
the form of a tree structure where each segmentation path represents a unique path
5       through the tree structure. The region within the initial segmentation map 203 that
occurs before the segmentation front 720 and 735 is classified as lesion and the
region after the segmentation front 720 is classified as vessel. The segmentation
front 735 can be used to approximately demark the boundary between the lesion
and the lung wall. The region within the initial segmentation map 203 after
10      segmentation front 735 is classified as normal anatomy. Unfortunately, these
methods to determine the boundary between the lesion and normal anatomy (lung
wall and mediastinum) are too restrictive and often fail to produce desirable
results. A primary reason is that such approaches are overly simplistic and do not
account for the local geometry, or the variability of surfaces within a volume.

15              Referring to Figures 9a and 9b that show a 3D representation of a
surface patch of the lung wall. In a healthy state the lung cavity (parenchyma) and
the lung wall are adjacent and the boundary between these two is a boundary
surface 900 that can be considered as topologically smooth. While this surface is
smooth, it does not imply that any region on the surface can be modeled as a plane
20      or low degree polynomial surface. If a lesion 910 is attached to this surface the
region of attachment 930 can be considered as a "hole" in the normal healthy
surface. The boundary of this hole is a closed non-self intersecting curve 940. It
then becomes necessary to reconstruct or interpolate a surface across this hole in
order to accurately determine the boundary between the lesion and lung wall.
25      Scattered data surface reconstruction/interpolation methods can be used to
reconstruct or interpolate a surface across this hole.

Surface reconstruction/interpolation using radial basis functions
RBF can be used to determine the boundary between the lesion and normal
anatomy for situations where a plane or a low degree polynomial surface cannot
30      sufficiently fit the topology of the dividing surface. Traditional surface
reconstruction creates a height field (or depth map) in order to fit a set of data
points (see J.C. Carr, et. al., "Surface Interpolation with Radial Basis Functions

for Medical Imaging," IEEE Transactions on Medical Imaging, Vol. 16, No. 1,
February 1997, pp 96-107). Height fields are parametric surfaces in that two
coordinates can uniquely give any position on the surface patch. Thus, height
field is a single valued function of two variables (2-D) $f : \Re^2 \rightarrow \Re$, where the
5    data at which the function values are known can be scattered, e.g., not collected on
a regular grid.

The function $f$ is approximated by $g : \Re^2 \rightarrow \Re$, given the values
$\{f(\mathbf{x}_i) := 1,2,...,n\}$, where $\{\mathbf{x}_i\}$ is the set of (x, y) coordinates of voxels on the
boundary between the lung parenchyma and normal anatomy. The interpolating
10   parametric function $g$ using radial basis functions is given by

$$g(\mathbf{x}) = \sum_{i=1}^{n} w_i \phi(\|\mathbf{x} - \mathbf{x}_i\|) + p(\mathbf{x}) \qquad (2)$$

where $w_i$ are the weights, $\mathbf{x}_i$ are the location of the boundary constraints (see
above), $\phi(\|\mathbf{x} - \mathbf{x}_i\|)$ is a radial basis function centered at $\mathbf{x}_i$, and $p(\mathbf{x})$ is a low
degree polynomial. The weights $w_i$ are determined by requiring that g satisfy the
15   following

$$g(\mathbf{x}_i) = f(\mathbf{x}_i) \qquad\qquad i = 1,2,3,....,n. \qquad (3)$$

In some situations it is necessary to transform the local coordinate system of the
surface patch to ensure that the surface patch represents a single valued function
and/or to maximize the domain of the surface to ensure an accurate interpolating
20   function (see Figure 10). For example, the surface patch 1010 represents a height
field that is not singled value function with a very restricted domain. Upon
transformation of the surface patch 1010 to 1020 a singled value function is
obtained with a maximized domain.

Some typical examples of radial basis functions are given below:

25

$$\phi(r) = \exp(-\alpha r^2)$$

$$\phi(r) = r$$

$$\phi(r) = r^2 \log(r)$$

$$\phi(r) = \sqrt{r^2 + c^2}$$

where $a$ and $c$ are positive constants.

The use of height fields is a barrier to creating surfaces of arbitrary

5    topology, especially in cases where two coordinates cannot uniquely give any

position on the surface patch (i.e. the height field is not single valued). To

overcome the limitations of a parametric surface, an interpolating implicit surface

method can be used to generate a boundary between the lesion and normal

anatomy. Traditional interpolating surfaces use a function with a 2D domain to

10   create a parametric surface, whereas the interpolating implicit method uses a

function with a 3D domain to specify the location of the implicit surface. The

implicit surface is defined as an isosurface (or level set) of a function

$f : \Re^3 \to \Re$ where the surface is defined at 3D location at which $f(\mathbf{X}) = 0$. The

implicit function takes on positive (negative) values for points that are below the

15   surface or are contained within a closed surface and negative (positive) values for

points above or are outside the closed surface.

The interpolating implicit function $g$ is given by

$$g(\mathbf{x}) = \sum_{i=1}^{n} w_i \phi(\|\mathbf{X} - \mathbf{X}_i\|) + p(\mathbf{X}) \qquad (4)$$

where $w_i$ are the weights, $\mathbf{X}_i$ are the 3D location of the constraints (see below),

20   $\phi(\|\mathbf{X} - \mathbf{X}_i\|)$ is a radial basis function centered at $\mathbf{X}_i$, and $p(\mathbf{X})$ is a low degree

polynomial.

For the implicit surface method it is necessary to specify both zero

value constraints (boundary) through which the surface must pass and positive

(negative) interior constraints and/or negative (positive) exterior constraints in

25   order to define the implicit function $g$. Alternatively, normal constraints can be

paired with a subset of the boundary constraints. Normal constraints are

generated by placing either a positive or negative constraint a small distance from

the boundary constraint in the direction of the surface normal. The magnitude of

the positive/negative constraints can be set either to +1 /-1 or to it's signed

30   distance from the closest boundary constraint. Figure 12 shows the location of the

boundary constraints 1210, interior and exterior constraints 1220 and normal
constraints 1230 for a 2D slice of the lesion attached to normal anatomy. Also
shown in Figure 12 are the segmentation fronts used to generate the constraints.

The weights $w_i$ are determined by requiring that g satisfy the
5    following

$$g(\mathbf{X}_i) = f(\mathbf{X}_i) \qquad i = 1,2,3,\ldots,n. \qquad (5)$$

The implicit surface can be determined (see R.K. Beatson, et.al., "Fast Solution of
the Radial Basis Function Interpolation Equations: Domain Decomposition
Methods," SIAM Journal of Scientific Computing, Vol. 22, No. 5, 2000, pp 1717-
10    1740) and the iso-surface of points having an interpolation value of zero can be
readily extracted using a method such as Marching Cubes (see W.E. Lorensen and
H.E. Cline, "Marching Cubes: A High Resolution 3D Surface Construction
Algorithm," Computer Graphics, Vol. 21, No. 3, 1987, pp 163-169).

A partition of unity strategy (see O. Schall, et. al., "Surface from
15    Scattered Points: A Brief Survey of Recent Developments," in 1st International
Workshop towards Semantic Virtual Environments, Villars, Switzerland,
MIRAlabs, 2005, pp 138-147) can be used to improve both the surface
reconstruction accuracy and computationally efficiency of the aforementioned
scattered data surface reconstruction techniques. The main idea of the partition of
20    unity (POU) approach is to divide the global domain of interest into smaller
overlapping domains where the problem is solved locally. The decomposition of
the data set into smaller subsets leads to a reduction in the computational
complexity of the surface fitting algorithms. Distant data samples do not contain
information needed for local approximation of the surface. The surface is
25    reconstructed on each subdomain separately, and the local surfaces are blended
together using a weighted sum of the local domain solutions

$$g(\mathbf{X}) = \sum_{i=1}^{m} w_i(\mathbf{X}) g_i(\mathbf{X}) \qquad (6)$$

where $g_i(\mathbf{X})$ is the locally reconstructed surface for $i = 1,2,3\ldots m$ subdomains and
the weights $w_i(\mathbf{X})$ are smooth functions and sum up to one everywhere in the
30

domain $\sum_{i=1}^{m} w_i = 1$.

Moving least squares MLS (see J. Wang and M. Olivera, "Filling

Holes on Locally Smooth Surfaces Reconstructed from Point Clouds," Image and

Vision Computing, Vol. 25, 2007, pp 103-113) provides another class of solution

5       for the problem of fitting a surface to scattered data. A scattered data surface

reconstruction technique closely related to partition of unity is the moving least-

squares method. MLS is an extension of the well known least squares LS

technique to fit a surface to a given set of data points. The term 'moving' refers to

the various weighting of the points in calculating their contributions to the

10      solution at different locations. The least squares approximation obtains a globally

defined function $g(\mathbf{X})$ that approximates the given the values $f_i$ at locations

$\mathbf{X}_i$ in at least squares sense. The function $g(\mathbf{X})$ is determined by the following

minimization problem

$$\min_{g \in \Pi_m^d} \sum_i \|g(\mathbf{X}_i) - f_i\| \qquad (7)$$

15      where $g$ is taken from $\Pi_m^d$, the space of polynomials of total degree $m$ in $d$ spatial

dimensions. The weighted least squares WLS formulation obtains a globally

defined function $g(\mathbf{X})$ by minimizes the following:

$$\min_{g \in \Pi_m^d} \sum_i w_i \|g(\mathbf{X}_i) - f_i\| \qquad (8)$$

where the errors are weight by $w_i$. The partition of unity strategy can be applied

20      to both the LS and WLS methods. The MLS formulation uses a WLS fit to

compute and evaluate for individual points in the domain. The function $g_{\mathbf{X}}(\mathbf{X})$ is

determined at each location $\mathbf{X}$ by the following minimization problem

$$\min_{g \in \Pi_m^d} \sum_i w_i(\mathbf{X}) \|g_{\mathbf{X}}(\mathbf{X}_i) - f_i\| \qquad (9)$$

25      where the weights $w_i$ is a radial function that depends upon the distance between $\mathbf{X}$

and the positions of the data points $\mathbf{X}_i$. Compared to LS and WLS methods, which

create a given polynomial surface, MLS computes a local polynomial fit continuously over the entire domain and blends them together. Thus, the MLS can fit the topology of higher order surfaces. The MLS method can be applied to both implicit and parameter surfaces.

5          Another surface useful for determining a boundary between the lesion and normal anatomy is the surface of minimal area that contains known boundary constraint voxels. This is commonly referred to as a minimal surface. The topic of minimal surfaces has a long history in mathematics and differential geometry. A means to compute such a surface (see D. L. Chopp, "Computing

10    Minimal Surfaces via Level Set Curvature Flow," Journal of Computational Physics, Vol. 91, 1994 pp. 77-91) from a set of known boundary constraints (voxels) utilizes a computational method commonly referred to as level-set methods. The approach begins with a set of voxels on the boundary between the lung parenchyma and normal anatomy that are connected in a natural manner to

15    form a space curve, i.e., a closed curve $\Gamma$ in the 3-dimensional space. If a surface is formed with the aforementioned space curve being its boundary $\Gamma$, then the surface may represent a separation between the so-call normal tissue and tissue belonging to the lesion. However, there are an infinite number of such surfaces. One surface of particular note is such a surface with the minimal surface area, the

20    so-called minimal surface. An equivalent property of these surfaces is that each point on the surface has zero mean curvature. An initial surface whose boundary is $\Gamma$, is evolved using mean curvature with the boundary of the evolving surface always given by $\Gamma$. The change in the surface is governed by the partial differential equation

25
$$\frac{dx(t)}{dt} \cdot n(x(t)) = \kappa(x(t)) \qquad (10)$$

where $\kappa(x(t))$ is the mean curvature at the point $x(t)$ and $n(x(t))$ is the normal of the surface at $x(t)$. The partial differential equation is solved using a level set method (see J.A. Sethian, "Level Set Methods and Fast Marching Methods", Cambridge University Press, 1999) in an iterative process that continues until

30    convergence is reached, i.e., when the local mean curvature is zero.

If the segmentation front path analyzer 320, determines that a segmentation front path has penetrated into the normal anatomy, such as the lung wall or mediastinum, it signals the segmentation map refiner 330 to invoke normal anatomy/lesion separator 1300. The details of a potential normal anatomy/lesion

5      separator 1300 are depicted in Figure 13. In the determine surface constraints step 1305, the set of surface constraints, i.e. voxels, needed to generate the normal anatomy/lesion boundary surface are determined. The segmentation fronts of the aforementioned segmentation front path that have been identified as being internal to the normal anatomy are used to generate the surface constraints. Voxels

10     associated with the identified segmentation fronts that are inactive (or frozen) form the boundary between the lung parenchyma and normal anatomy. These voxels form the set of possible surface boundary constraints. Voxels in the identified segmentation fronts that are not inactive, i.e. voxels that have been classified in the initial segmentation map, correspond to the set of possible

15     positive constraints. Voxels neighboring the boundary constraints that have been classified as background in the initial segmentation map 203 and the initial seed point 205 correspond to the set of possible negative constraints. Normal constraints are obtained by calculating the surface normal for the boundary constraints and choosing from the set of possible negative and positive constraints

20     voxels that are close to the boundary and are in the direction of the normal. For the minimal surface only one of the identified segmentation fronts is considered for the surface boundary constraints. The inactive (or frozen) voxels of the chosen segmentation form the boundary between the lung parenchyma and normal anatomy. These voxels can be connected in a natural manner to form a space

25     curve, i.e., a closed curve $\Gamma$ in the 3-dimensional space. Figures 11a, 11b, and 11c show a schematic representation of the segmentation fronts 1110, 1120, and 1130 at different path length used to generate the surface constraints. Figure 12 shows the location of the boundary constraints 1210, interior and exterior constraints 1220 and normal constraints 1230 for a 2D slice of the lesion attached

30     to normal anatomy. Also shown in Figure 12 are the segmentation fronts 1240 used to generate the constraints.

For the parametric surface, the local orientation of the normal
anatomy around the lesion is determined. The surface orientation is used to
transform the coordinate system of the identified boundary constraint voxels so as
to maximize the domain of the height field and/or form a valid height field (see

5      Figure 10). The appropriate orientation (transformation) can be obtained either by
generating a plane whose normal is consistent with a majority the surface normal
of the boundary constraints or by a eigenvector analysis of the covariance matrix
of the boundary constraints locations.

The determine type of surface step 1310, determines the preferred

10     type of surface for generating a boundary between the lesion and normal anatomy.
Potential choices for the boundary surface are a segmentation front, a 3D plane, a
low degree parametric polynomial, an interpolating RBF parametric, an
interpolating RBF implicit, or minimal surface. The segmentation front paths are
analyzed to determine which surface is appropriate. The decision is based upon a

15     number of factors such as the confidence in the constraint data, number
(density/sparsity) of boundary constraints, validity of the constraint data
conforming to a singled valued height field, and the complexity/ambiguity of the
connection of the nodule to the underlying surface. One indicator that the
complexity/ambiguity is potentially high is when the segmentation front path

20     analyzer 330 indicates that multiple segmentation front paths have independently
connected to the surface. In a preferred implementation, the interpolating
parametric or low degree parametric polynomial surface is chosen if there are a
sufficient number of boundary constraints available and the height field is a single
valued function. An interpolating implicit surface is preferably chosen when there

25     are a sufficient number of constraints (boundary, interior, exterior, and normal)
available and the height field is poorly behaved and/or the complexity/ambiguity
of the surface is high. Alternatively, the minimal surface is preferred when the
there are a sparse number of boundary constraints and/or the
complexity/ambiguity of the surface is high.

30               In the construct surface step 1320, the aforementioned surface
constraints are used to construct the appropriate surface. For the parametric or
implicit surface, the interpolating parametric function $g$ (Equation 2) or implicit

surfaces the interpolating implicit function *g* (Equation 4) is determined and for the minimal surface the partial differential equation (Equation 6) is solved. In the generate lesion/normal anatomy boundary step 1330, the boundary surface between the lesion and normal anatomy is determined and used to modify the

5    initial segmentation map 203 to generate the final segmentation map 204. For the aforementioned surface methods, once the boundary surface is determined, the initial segmentation map 203 is separated into at least two disjoint subsets. The voxels in the subset containing the initial seed point are classified as belonging to the lesion, while others are classified as belonging to normal anatomy.

10   Additionally for the implicit surface method, those voxels in the segmentation map that interpolate to negative values are considered lesion voxels and those that interpolate to positive values are considered to belong to the normal anatomy.

# PARTS LIST

| | |
|---|---|
| 10a | image capture device |
| 10b | DR capture device |
| 42a | electronic display device |
| 42b | electronic display device |
| 44a | input control device |
| 44b | input control device |
| 60 | mobile computer |
| 110 | communications network |
| 120 | diagnostic workstation computer |
| 140 | image archive computer |
| 150 | segmentor |
| 201 | source digital images |
| 202 | volume image |
| 203 | initial segmentation map |
| 204 | segmentation map |
| 205 | seed point |
| 206 | image processing parameters |
| 207 | reported volume |
| 208 | segmentation front paths |
| 209 | rendered segmentation map |
| 220 | slice image assembler |
| 230 | lesion segmentor |
| 240 | image renderer |
| 250 | volume estimator |
| 310 | initial lesion segmentor |
| 312 | grow segmentation step |
| 313 | classify the segmentation front into active and inactive fronts step |
| 314 | partition active segmentation front into connected fronts step |
| 315 | calculate features for each connect front step |
| 316 | link connected fronts with segmentation front paths step |
| 317 | continue segmentation step |

320     segmentation front path analyzer

330     segmentation map refiner

500     grid

510     current segmentation map

510a    segmentation map

520     set of voxels

530     set of voxels

540     active segmentation front

540a    labeled active front

540b    labeled active front

550     inactive segmentation front

610     juxta-pleural lesion

620     juxta-vascular lesion

630     juxta-vascular lesion

640     lesion containing a spiculated tentacle

705     segmentation front

710     segmentation front

715     segmentation front

720     segmentation front

725     segmentation front

730     segmentation front

735     segmentation front

740     segmentation front

745     segmentation front

900     boundary surface

910     lesion

930     hole in surface

940     closed non-self intersecting curve

1010    surface patch

1020    surface patch

1110    3D segmentation front

1120    3D segmentation front

1130    3D segmentation front

1210    boundary constraint

1220    interior and exterior constraints

1230    normal constraint

1240    segmentation front

1300    normal anatomy/lesion separator

1305    determine surface constraints step

1310    determine type of surface step

1320    construct surface step

1330    generate lesion/normal anatomy boundary step

**CLAIMS:**

1.      A method of segmenting a lesion from normal anatomy in a 3-dimensional image comprising the steps of:

        a) receiving an initial set of voxels that are contained within the lesion to be segmented;

        b) growing a region which includes the lesion from the initial set of voxels;

        c) identifying a second set of voxels on a surface of the normal anatomy;

        d) determining a surface containing the second set of voxels which demarks a boundary between the lesion and the normal anatomy; and

        e) classifying voxels which are part of the lesion.

2.      A method as in claim 1 wherein said step of growing a region comprises a segmentation front analysis.

3.      A method as in claim 2 wherein segmentation front analysis comprises a fast marching method.

4.      A method as in claim 2 wherein said step of identifying a second set of voxels is derived from the segmentation front analysis.

5.      A method as in claim 2 wherein the demarcation boundary is determined by a scattered data surface reconstruction method.

6.      A method as in claim 5 wherein the scattered data surface reconstruction is by a low degree polynomial surface.

7.      A method as in claim 5 wherein the scattered data surface reconstruction is achieved by interpolating radial basis function.

8.      A method as in claim 7 wherein the interpolating function is a parametric function.

9.      A method as in claim 7 wherein the interpolating function is an implicit function.

10.      A method as in claim 5 wherein the scattered data surface reconstruction method utilizes a partition of unity.

11.      A method as in claim 5 wherein the demarcation boundary is determined using a moving least squares method.

12.      A method as in claim 5 wherein the demarcation boundary is a minimal surface.

13.      A method as in claim 1 wherein the demarcation boundary is determined by a scattered data surface reconstruction method.

14.      A method as in claim 13 wherein the scattered data surface reconstruction is achieved by interpolating radial basis function.

15.      A method as in claim 14 wherein the interpolating function is a parametric function.

16.      A method as in claim 14 wherein the interpolating function is an implicit function.

17.      A method as in claim 13 wherein the scattered data surface reconstruction method utilizes a partition of unity.

18.      A method as in claim 13 wherein the demarcation boundary is determined using a moving least squares method.

19.    A method as in claim 13 wherein the demarcation boundary is a minimal surface.

5                   20.    A method as in claim 5 wherein the scattered data surface reconstruction method is determined by the segmentation front analysis.
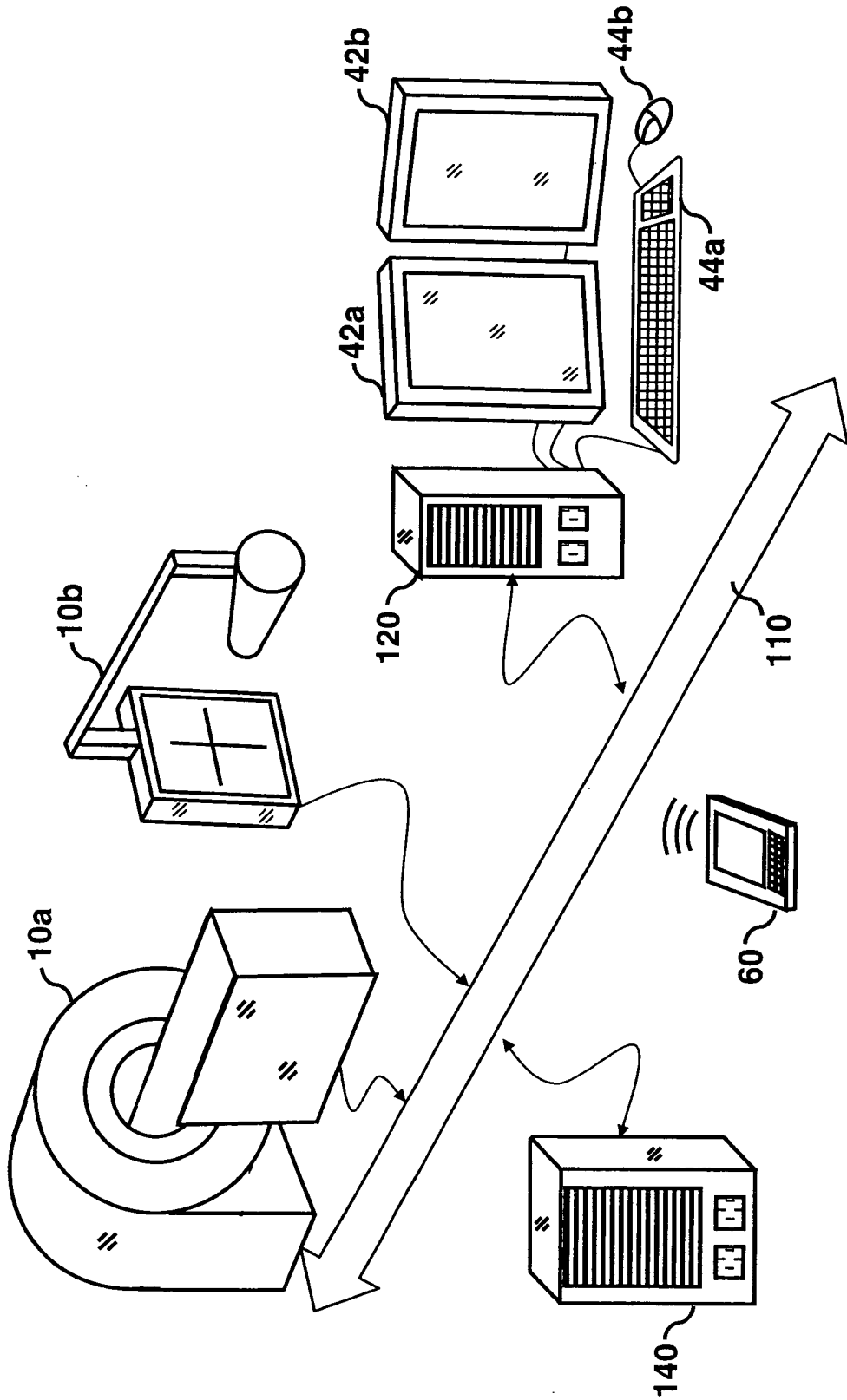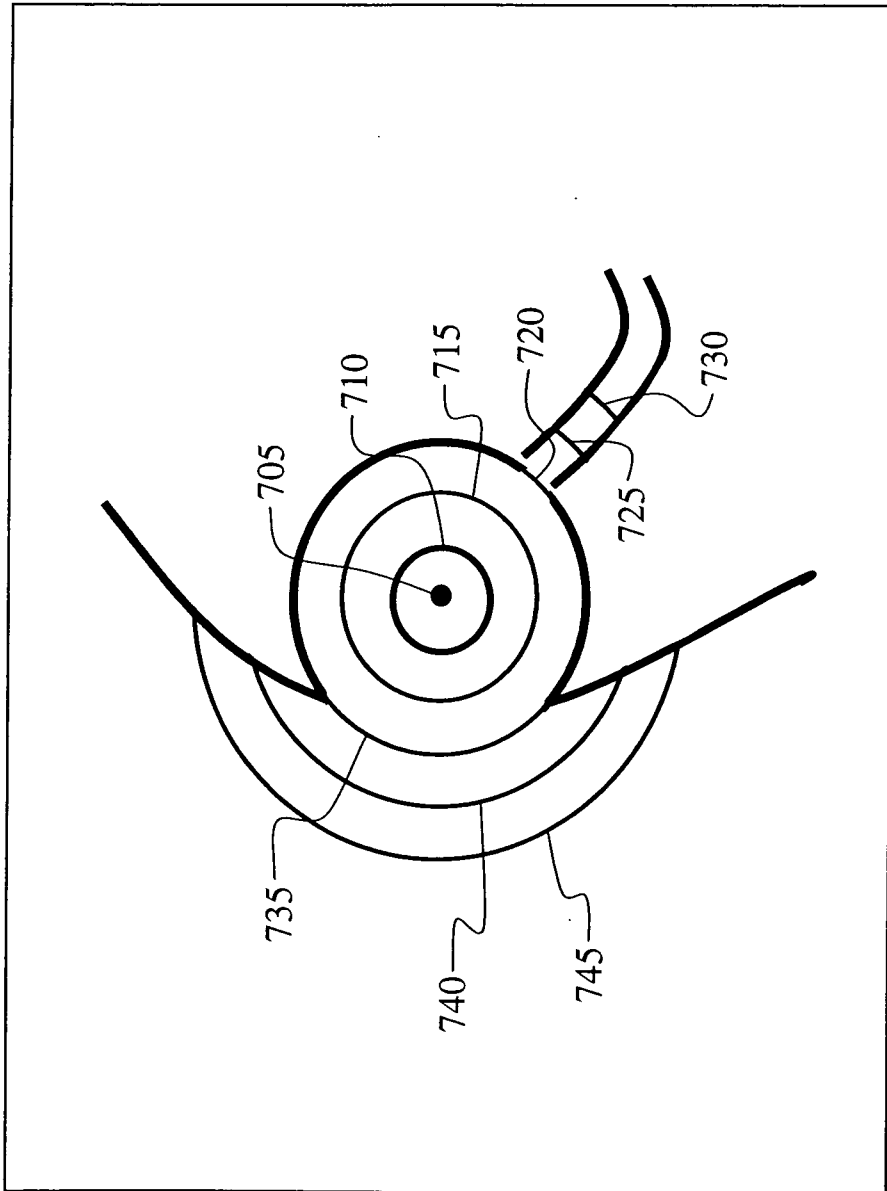
**FIG. 1**
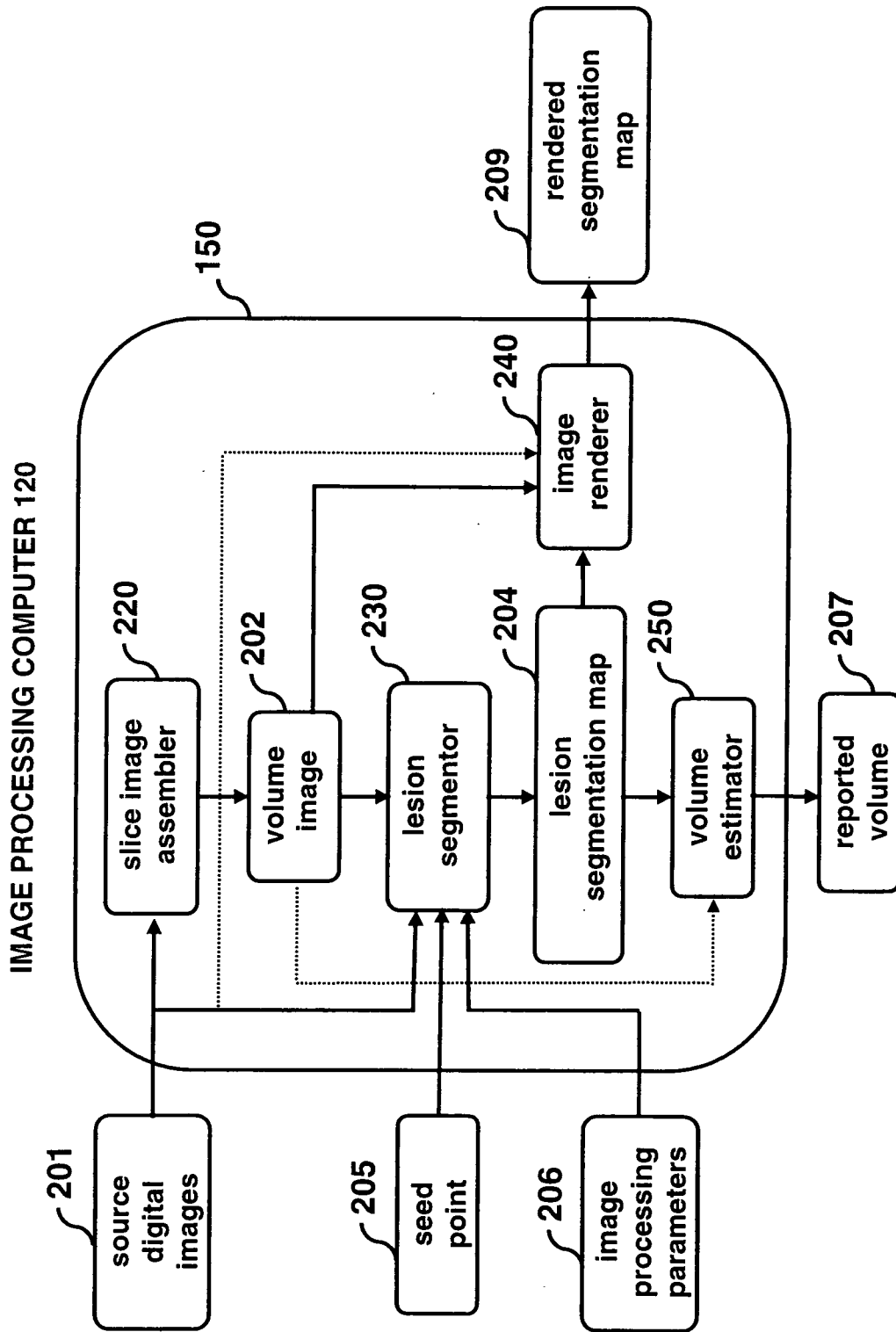
**FIG. 2**
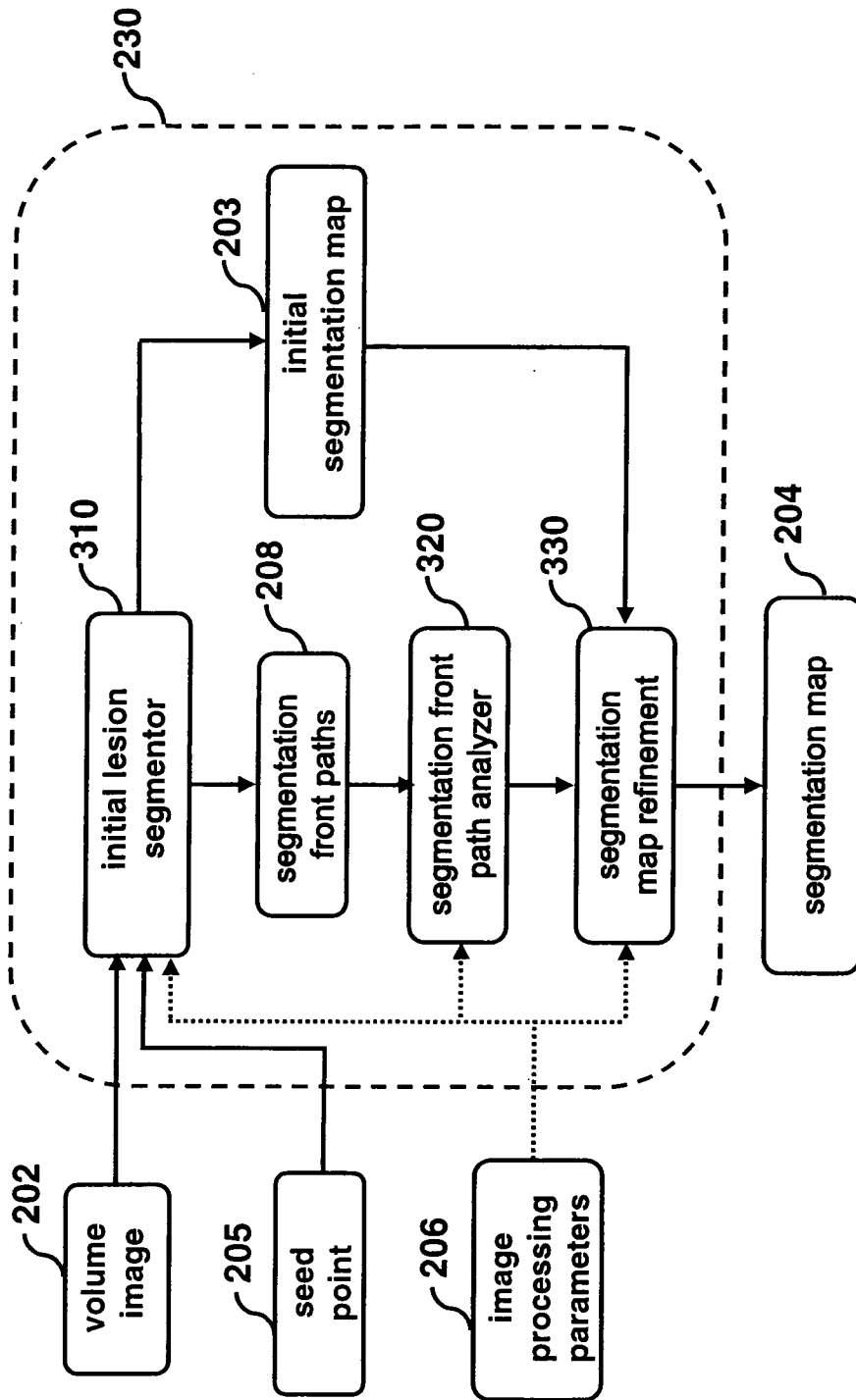
**FIG. 3**
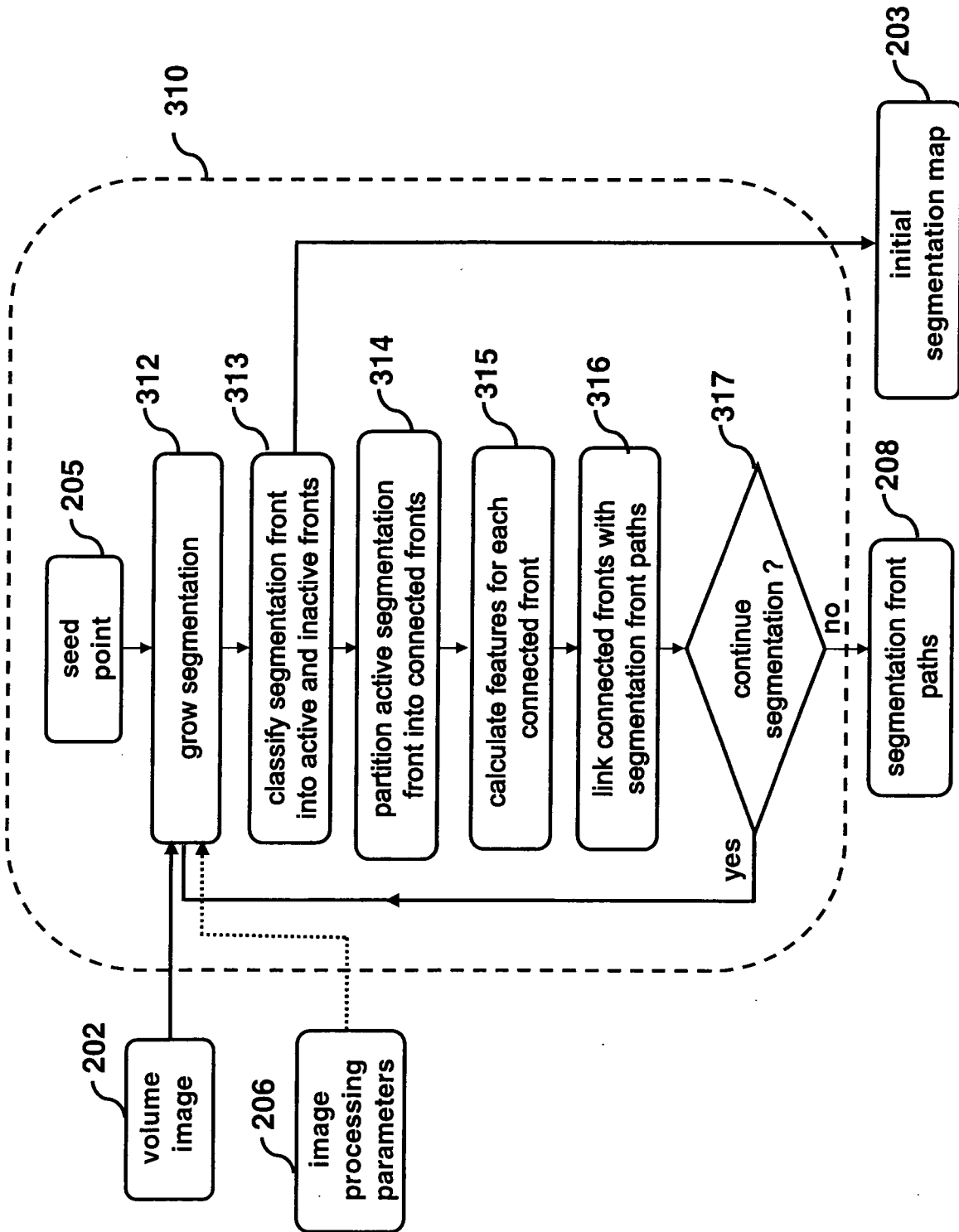
FIG. 4
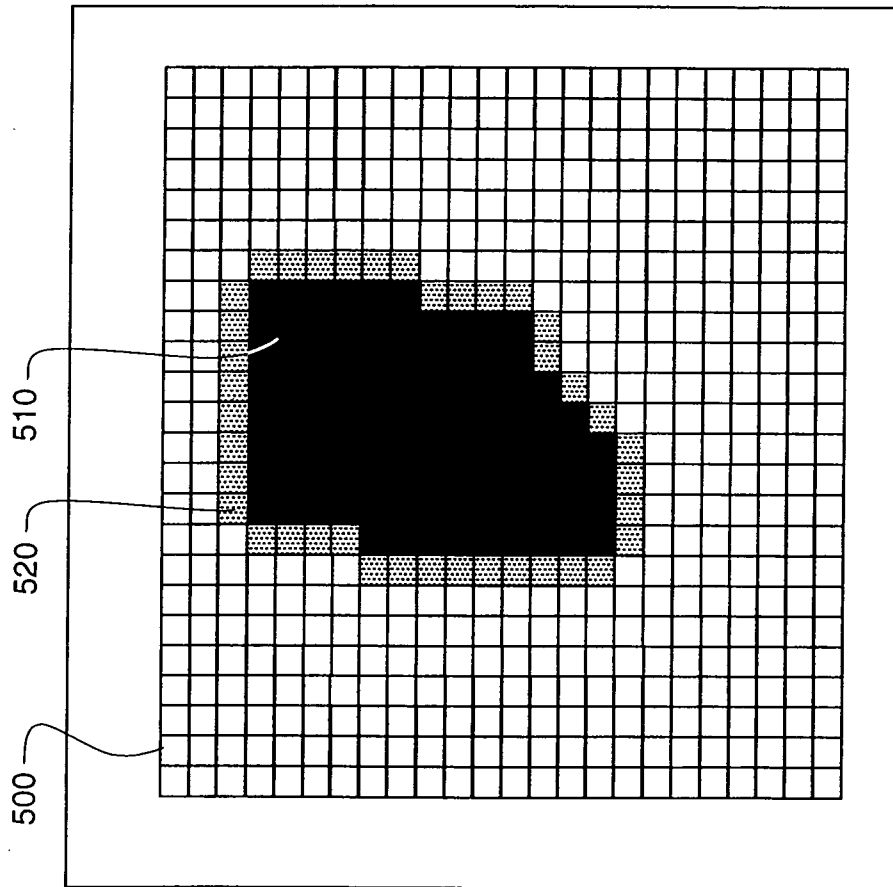
**FIG. 5a**
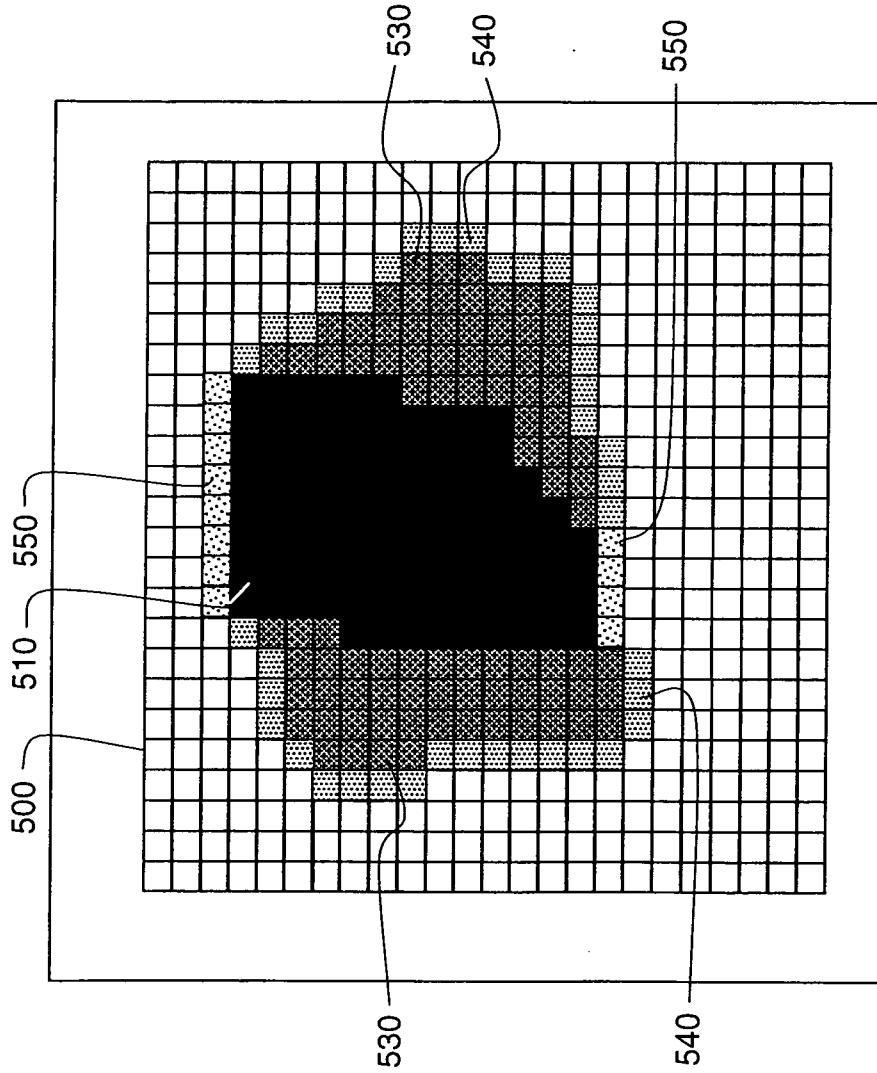
FIG. 5b
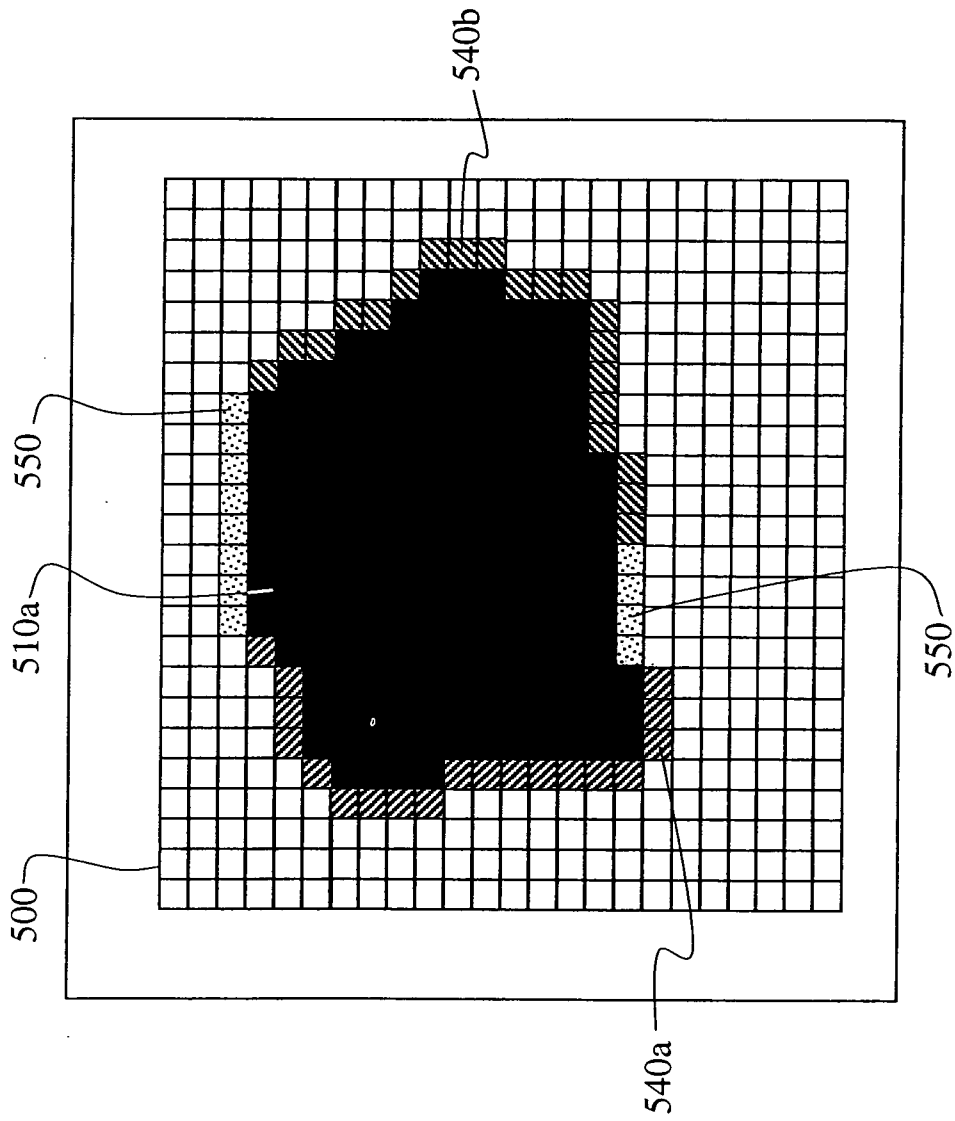
FIG. 5c
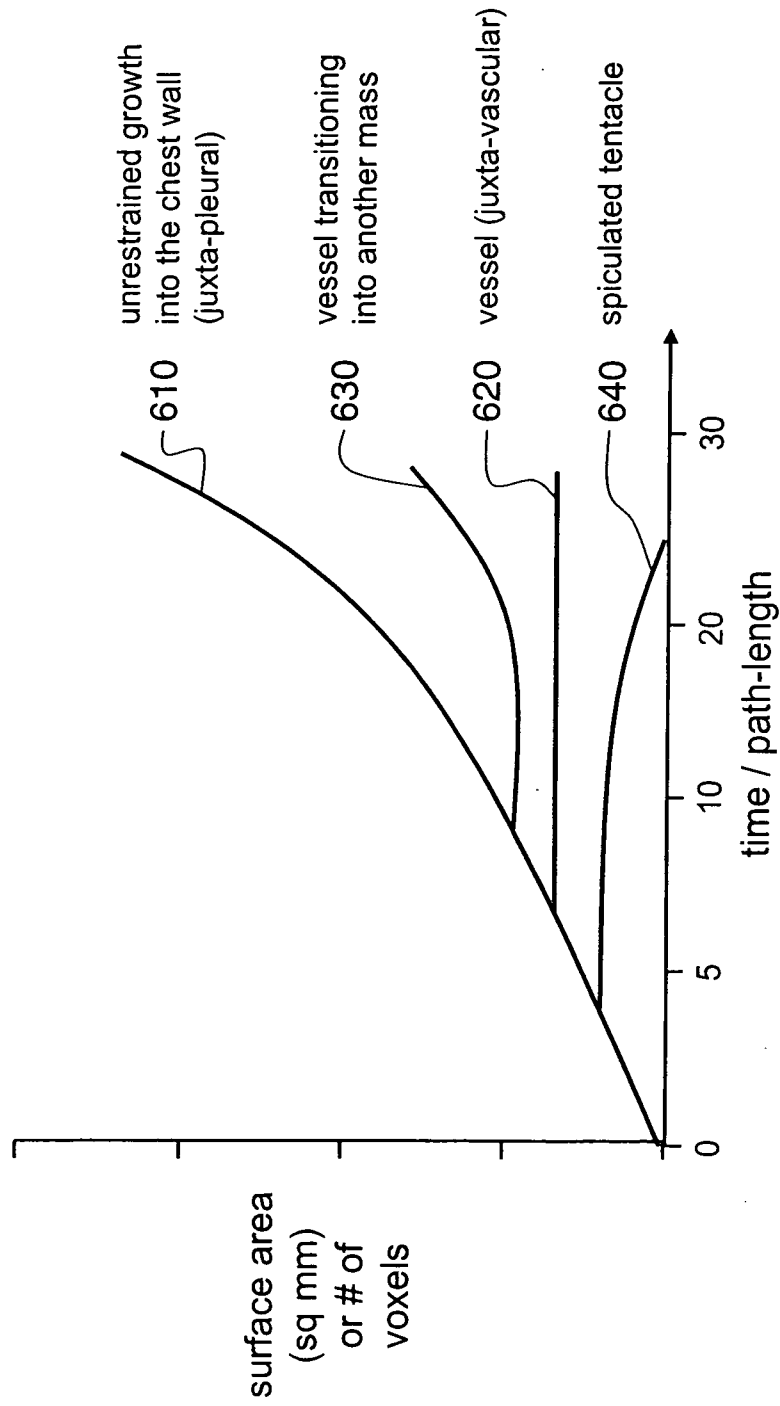
FIG. 6

**FIG. 7**
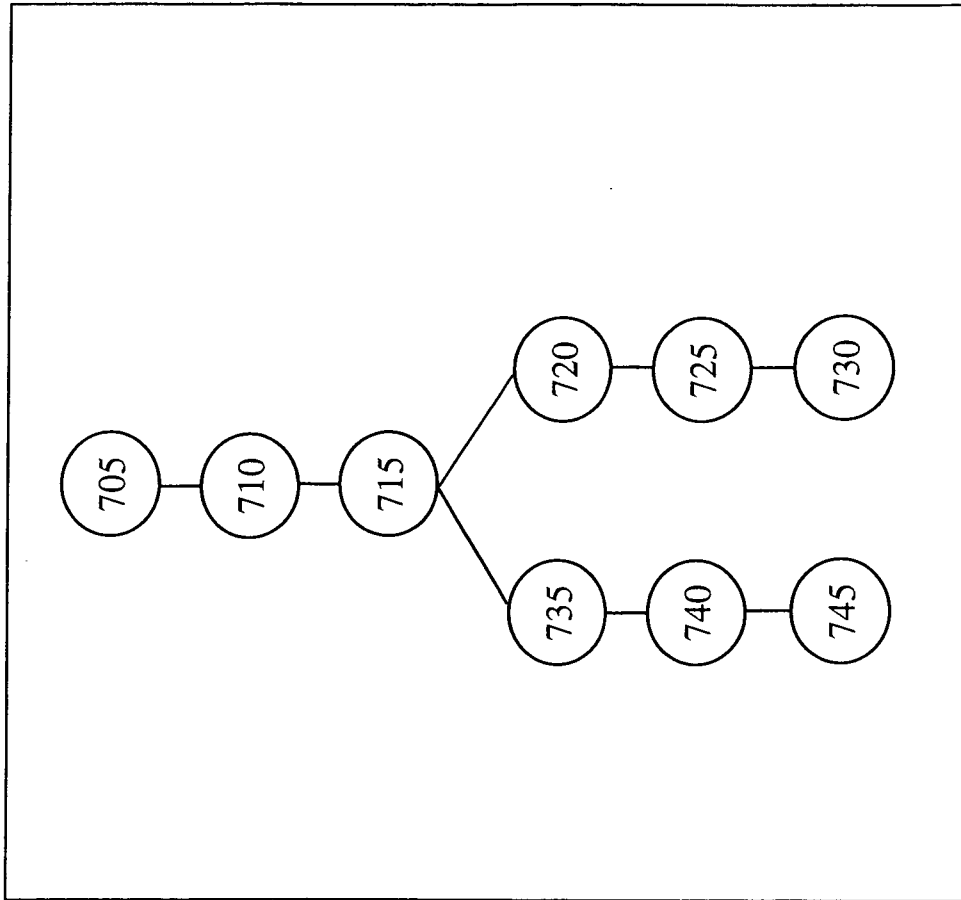
FIG. 8
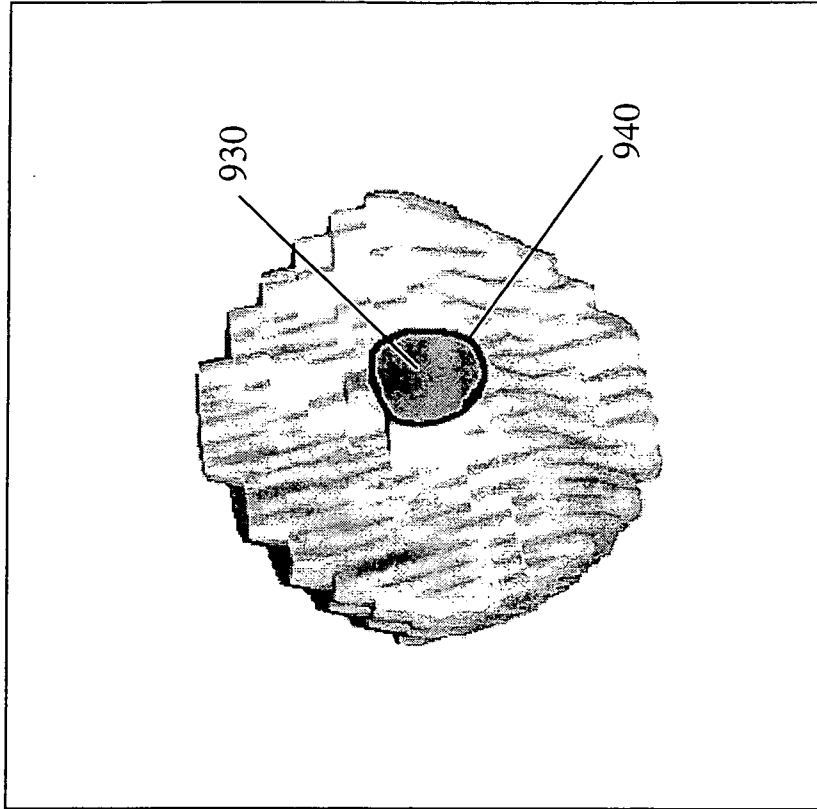
FIG. 9B
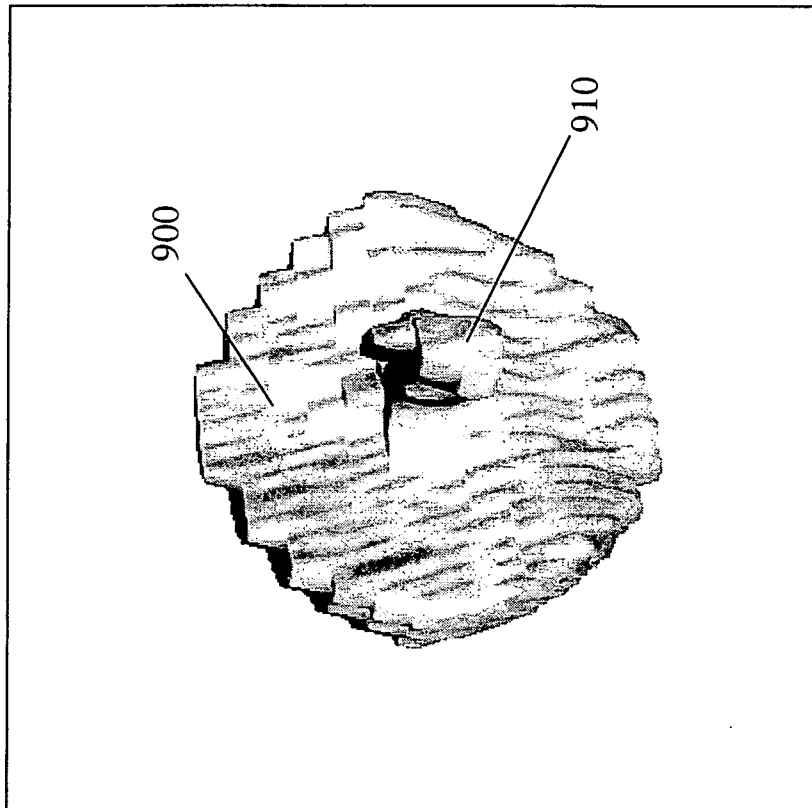


FIG. 9A
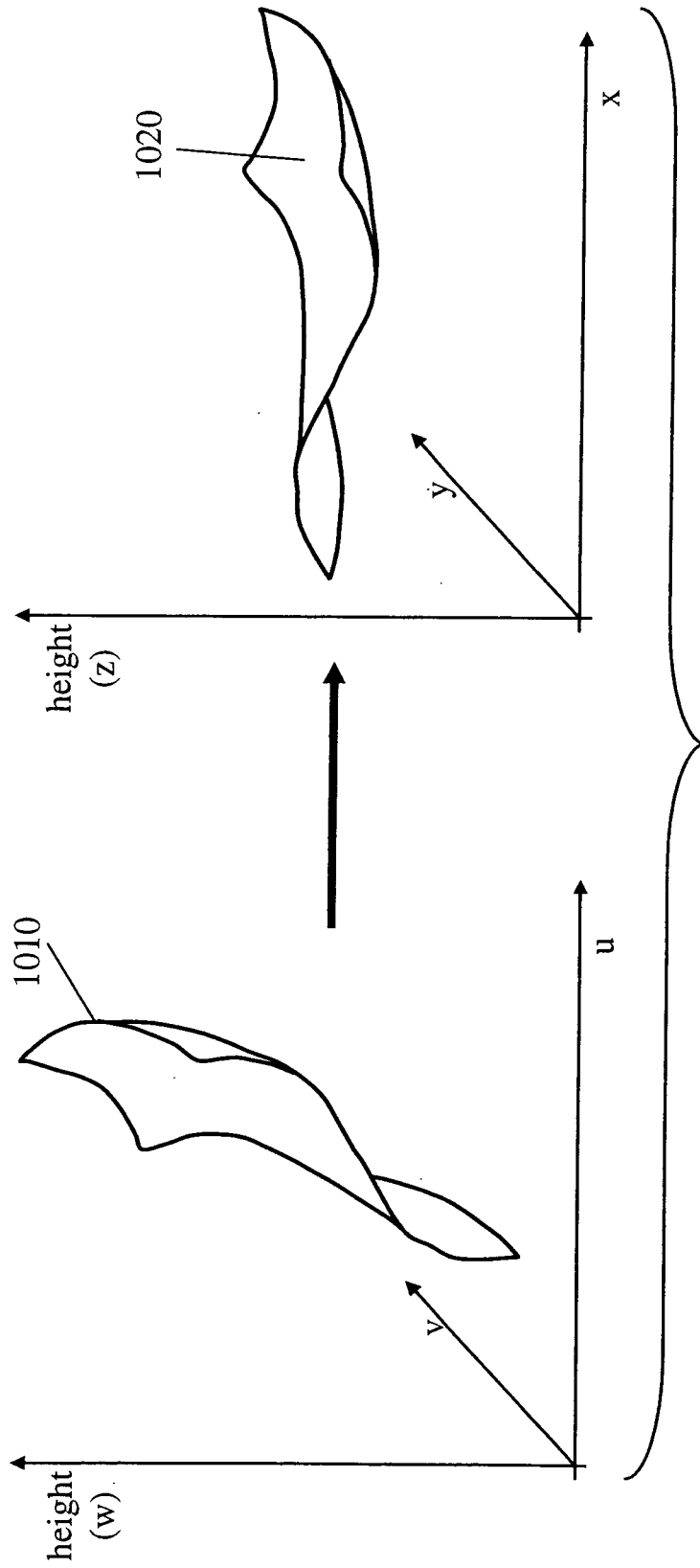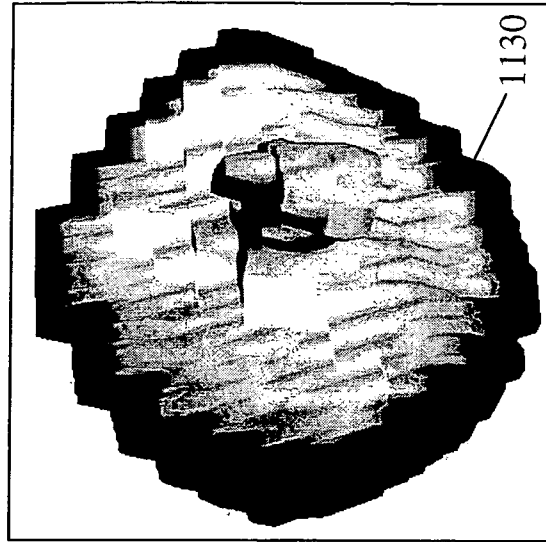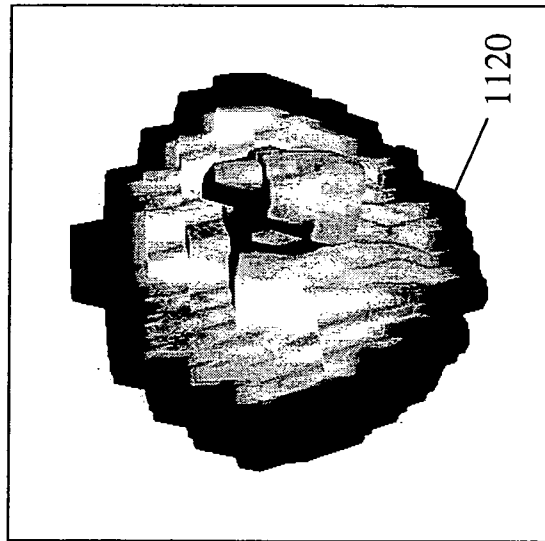
**FIG. 10**
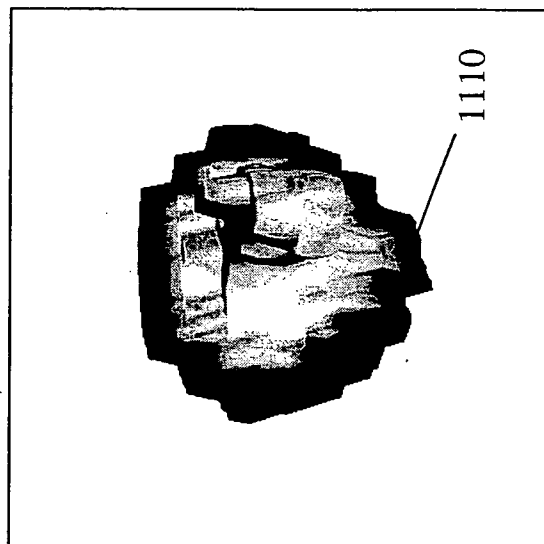
FIG. 11c



FIG. 11b



FIG. 11a

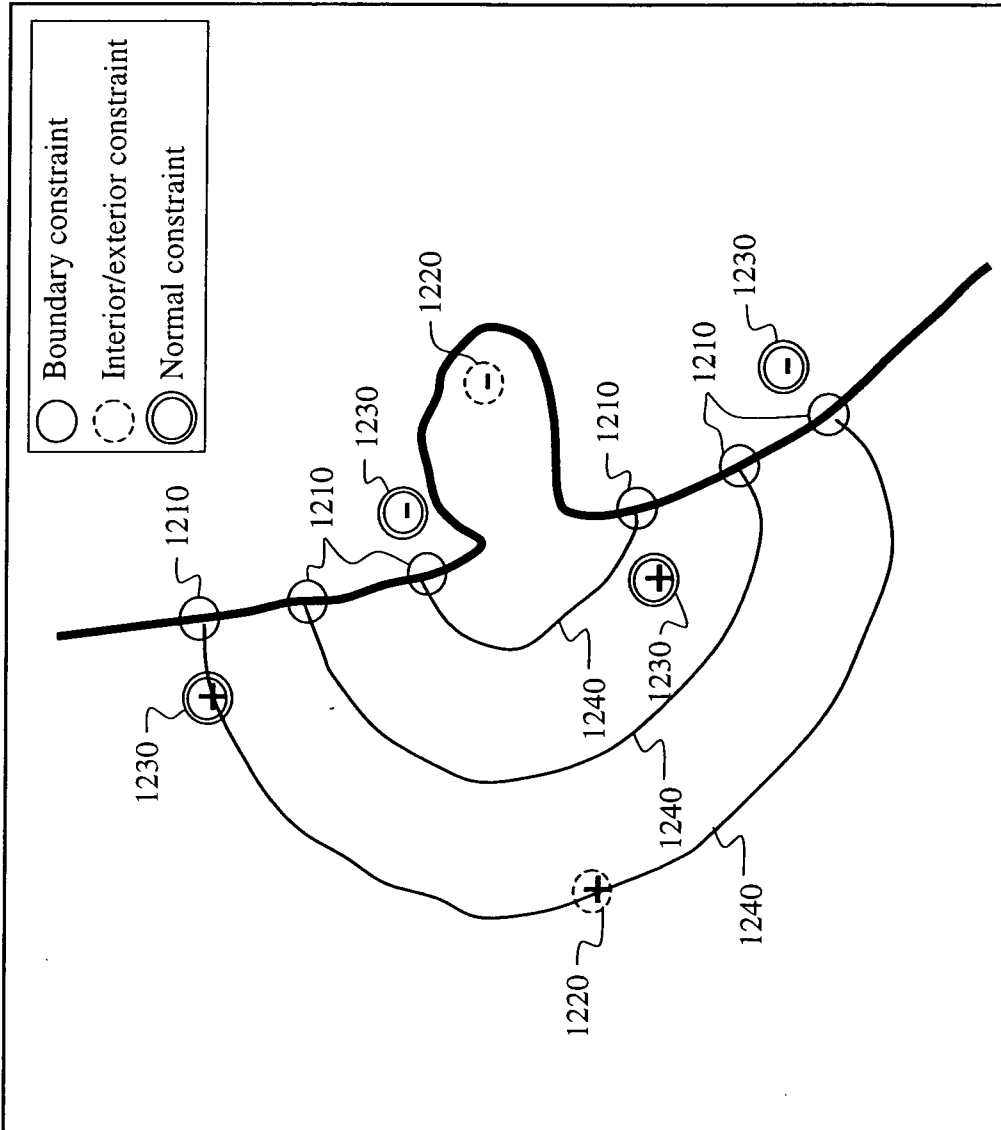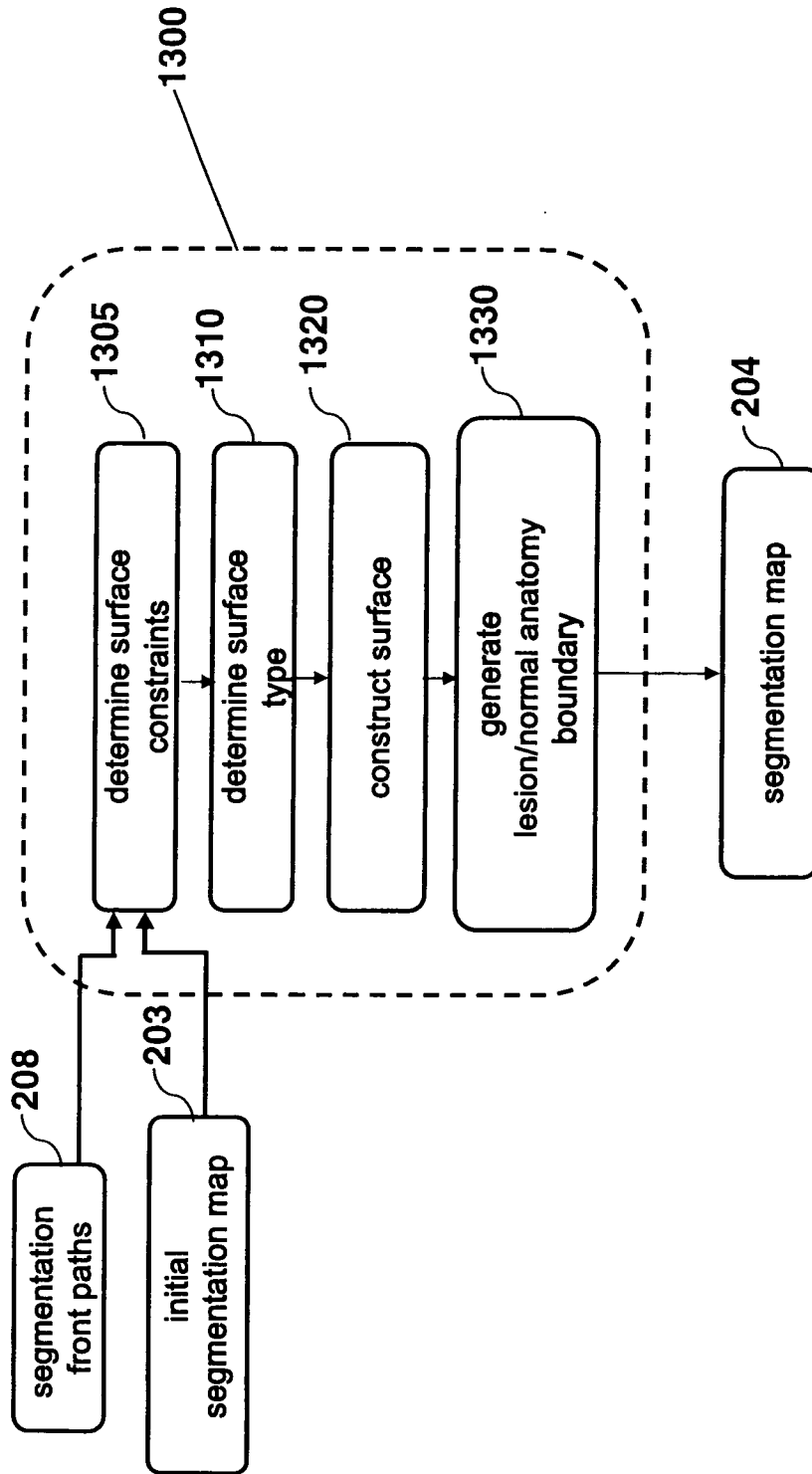FIG. 12

FIG. 13

# INTERNATIONAL SEARCH REPORT

**A. CLASSIFICATION OF SUBJECT MATTER**
INV. G06T5/00    G06T7/00

According to International Patent Classification (IPC) or to both national classification and IPC

**B. FIELDS SEARCHED**

Minimum documentation searched (classification system followed by classification symbols)
G06T

Documentation searched other than minimum documentation to the extent that such documents are included in the fields searched

Electronic data base consulted during the international search (name of data base and, where practical, search terms used)

EPO-Internal

**C. DOCUMENTS CONSIDERED TO BE RELEVANT**

| Category* | Citation of document, with indication, where appropriate, of the relevant passages | Relevant to claim No. |
|---|---|---|
| A | WO 2004/081874 A (SIEMENS MEDICAL SOLUTIONS [US]; JEREBKO ANNA [US]; KRISHNAN ARUN [US];) 23 September 2004 (2004-09-23) abstract; figures 1,4 page 3, line 27 - page 4, line 3 page 7, lines 8-28 page 9, lines 17-27 page 10, lines 14-30 page 13, lines 1-14 page 14, lines 6-23 <br><br> -/-- | 1-20 |

[X] Further documents are listed in the continuation of Box C.    [X] See patent family annex.

* Special categories of cited documents :

"A" document defining the general state of the art which is not considered to be of particular relevance
"E" earlier document but published on or after the international filing date
"L" document which may throw doubts on priority claim(s) or which is cited to establish the publication date of another citation or other special reason (as specified)
"O" document referring to an oral disclosure, use, exhibition or other means
"P" document published prior to the international filing date but later than the priority date claimed

"T" later document published after the international filing date or priority date and not in conflict with the application but cited to understand the principle or theory underlying the invention
"X" document of particular relevance; the claimed invention cannot be considered novel or cannot be considered to involve an inventive step when the document is taken alone
"Y" document of particular relevance; the claimed invention cannot be considered to involve an inventive step when the document is combined with one or more other such documents, such combination being obvious to a person skilled in the art.
"&" document member of the same patent family

| Date of the actual completion of the international search | Date of mailing of the international search report |
|---|---|
| 21 April 2008 | 29/04/2008 |

| Name and mailing address of the ISA/ <br> European Patent Office, P.B. 5818 Patentlaan 2 <br> NL – 2280 HV Rijswijk <br> Tel. (+31–70) 340–2040, Tx. 31 651 epo nl, <br> Fax: (+31–70) 340–3016 | Authorized officer <br><br> Casteller, Maurizio |
|---|---|

# INTERNATIONAL SEARCH REPORT

**C(Continuation).   DOCUMENTS CONSIDERED TO BE RELEVANT**

| Category* | Citation of document, with indication, where appropriate, of the relevant passages | Relevant to claim No. |
|---|---|---|
| A | US 6 246 784 B1 (SUMMERS RONALD M [US] ET AL) 12 June 2001 (2001-06-12) | 1-20 |
| A | abstract; claims 1,10,11<br>column 7, lines 16-40<br>column 8, lines 2-31<br>column 9, lines 44-59<br>column 10, lines 4-37<br>column 17, line 54 - column 18, line 34 | |
| A | LIXU GU ET AL: "3D Segmentation of Medical Images Using a Fast Multistage Hybrid Algorithm"<br>INTERNATIONAL JOURNAL OF COMPUTER ASSISTED RADIOLOGY AND SURGERY ; A JOURNAL FOR INTERDISCIPLINARY RESEARCH, DEVELOPMENT AND APPLICATIONS OF IMAGE GUIDED DIAGNOSIS AND THERAPY, SPRINGER-VERLAG, BE,<br>vol. 1, no. 1, 1 March 2006 (2006-03-01),<br>pages 23-31, XP019360745<br>ISSN: 1861-6429<br>abstract<br>page 24, right-hand column, line 25 - page 25, right-hand column, line 12<br>page 27, left-hand column, lines 3-44 | 1-20 |
| A | COLLIOT ET AL: "Segmentation of focal cortical dysplasia lesions on MRI using level set evolution"<br>NEUROIMAGE, ACADEMIC PRESS, ORLANDO, FL, US,<br>vol. 32, no. 4,<br>1 October 2006 (2006-10-01), pages 1621-1630, XP005644162<br>ISSN: 1053-8119<br>abstract<br>page 1622, left-hand column, line 35 - right-hand column, line 5<br>page 1624, right-hand column, lines 6-40 | 1-20 |
| A | RAJGURU N S ET AL: "Enhanced Level-Set Approach to Segmentation of 3-D Heterogeneous Lesions from Dynamic Contrast-Enhanced MR Images"<br>IMAGE ANALYSIS AND INTERPRETATION, 2006 IEEE SOUTHWEST SYMPOSIUM ON DENVER, CO MARCH 26-28 2006, PISCATAWAY, NJ, USA,IEEE, 26 March 2006 (2006-03-26), pages 71-75, XP010917528<br>ISBN: 1-4244-0069-4<br>abstract<br>paragraph [3.4.] | 1-20 |

2

# INTERNATIONAL SEARCH REPORT

Information on patent family members

| Patent document cited in search report | | Publication date | Patent family member(s) | | Publication date |
|---|---|---|---|---|---|
| WO 2004081874 | A | 23-09-2004 | DE 112004000381 | T5 | 24-05-2006 |
| | | | DE 112004000381 | B4 | 28-02-2008 |
| | | | JP 2006519634 | T | 31-08-2006 |
| | | | US 2004228529 | A1 | 18-11-2004 |
| US 6246784 | B1 | 12-06-2001 | US 6345112 | B1 | 05-02-2002 |